Soil Dynamics and Earthquake Engineering 187 (2024) 108989

Contents lists available at ScienceDirect

Soil Dynamics and Earthquake Engineering

journal homepage: www.elsevier.com/locate/soildyn

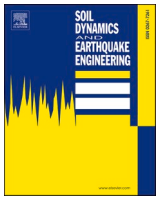

Estimation of effective damping ratio for cast-in-place tunnel-form system and evaluation of its role in performance point prediction

Vahid Mohsenian [a], Luigi Di-Sarno [b,c,*]

[a] Postgraduate Researcher, Department of Civil Engineering, University of Science and Culture, Tehran, Iran
[b] Department of Civil and Environmental Engineering, University of Liverpool, Liverpool, UK
[c] Department of Structures for Engineering and Architecture, University of Naples Federico II, Italy

ARTICLE INFO

Keywords:
Tunnel-form system
Effective damping ratio
Performance point
Probable performance interval
Capacity spectrum method
Displacement coefficient method
Displacement amplification factor

ABSTRACT

The extensive time and computational effort are primary challenges in nonlinear dynamic analysis of tunnel-form concrete systems. These challenges lead engineers to resort to simpler, pushover-based analyses, inherently based on estimating the seismic performance point of the system. Technical literature review indicates that no study has yet rigorously evaluated the accuracy of existing methods for estimating the performance point of tunnel-form systems. To eliminate potential ambiguities, in this study, the seismic performance point of the system under design basis earthquake (with a 475-year return period) has been calculated using three different methods (i.e., displacement coefficient, capacity spectrum, and displacement amplification factor), and compared with the results of accurate nonlinear time-history analysis. In the range of 5-, 7-, and 10-story models studied, the results indicate the inefficiency and insufficiency of the mentioned methods. Investigations reveal that while the capacity spectrum method provides better results, but its process is lengthy, and the displacement coefficient method significantly overestimates the performance point (with more than 80 % error). It was also evident that the displacement amplification factor underestimates the performance point and contradicts the direction of confidence. Based on observations, the use of all three methods for the tunnel-form system requires modifications. The calculated values of effective damping ratio for the tunnel-form system explicitly indicate type A behavior according to the ATC-40 classification. By presenting this parameter in a multi-level format, the shortcomings of both capacity spectrum and displacement coefficient methods are easily addressed. Referring to the results, the calculated value of the displacement amplification factor in the system exceeds the recommended value by the seismic design code, and by adjusting it, satisfactory responses can be obtained in the method based on the displacement amplification factor. Finally, introducing the "probable performance interval" parameter, recommending its use instead of the "performance point" parameter in assessments by pushover analysis is suggested. This parameter is applicable with all three mentioned methods and has been introduced in this study as a desirable factor in compensating for inherent uncertainties related to future earthquakes.

1. Introduction

Based on analytical studies, it is anticipated that cast-in-place tunnel-form systems exhibit desirable seismic performance [1,2]. Field investigations conducted after the Turkey earthquakes in 1999 and 2023 have somewhat validated this prediction [3,4]. Observations indicate relatively satisfactory seismic reliability of concrete buildings with tunnel-form systems (see Fig. 1).

So far, no specific seismic code has been formulated for tunnel-form systems. Despite clear performance differences, in the existing prescriptive regulations, tunnel-form system is still categorized under the category "Bearing wall" system [5].

In this integrated structural system, seismic performance is three-dimensional, stemming from the interaction of intersecting walls with each other and with slabs [3]. Considering both analytical and experimental studies, the failure mode in the system can be brittle [6,7].

Investigations have shown that the empirical relationships proposed by the seismic codes will provide inaccurate estimation of the fundamental period of vibration of the system [8–10]. To overcome this challenge, specific relationships have also been proposed for tunnel-form system [3,11].

The specific construction technique and the necessity of formwork

* Corresponding author. Department of Civil and Environmental Engineering, University of Liverpool, Liverpool, UK.
E-mail addresses: v.mohsenian@usc.ac.ir (V. Mohsenian), luigi.di-sarno@liverpool.ac.uk (L. Di-Sarno).

https://doi.org/10.1016/j.soildyn.2024.108989
Received 6 July 2024; Received in revised form 2 September 2024; Accepted 18 September 2024

Fig. 1. Examples of cast-in-place tunnel-form buildings after experiencing strong earthquakes and aftershocks: Turkey, 2023.

removal from the peripheral faces of the structure leads to high structural walls density in the central parts of the plan. Consequently, in many tunnel-form buildings, torsional stiffness is lower relative to lateral stiffness, and so their dominant behavior is of torsionally-flexible type [12]. However, studies have shown that accidental torsions resulting from asymmetric distributions of mass, stiffness and strength in the plan will not affect the seismic reliability of the system under design basis earthquake (return period of 475 years) [13]. In some studies, it is concluded that the requirements for the regularity of the system in the plan and height is excessively conservative [14,15]. Some studies have also shown that under design basis earthquake, a response modification factor of 4 will be appropriate for the system [16,17].

Investigations have also shown that the pulse directivity and flexibility of the base can be two factors contributing to the formation of unexpected failure modes in the system [18,19].

In the light of the interaction between intersecting walls and slab, modeling all elements using specific meshing is essential. Moreover, considering the significant role of coupling beams in increasing the lateral stiffness and strength of the system, excluding these elements from the model is impossible [20]. All these factors lead to an increase in the number of nodes in the computational model and, consequently, an increase in the computational cost and time.

The unique features of the system (significant seismic strength, cost reduction, high construction speed and safety for workers) have made it a popular option for mass construction in densely populated and seismic-prone areas. Since this industrialized technique is mostly used for high-rise buildings with spacious floor plans (see Fig. 1 again), nonlinear time-history analysis of such buildings is usually associated with a high computational volume and is very time-consuming [21].

This challenge encourages designers and engineers to take advantage of simpler pushover analysis, where the lateral load pattern and the target displacement (or performance point) are two essential principles.

In technical documents for estimating the target displacement of buildings under a specific earthquake, in addition to the displacement amplification factor method (C_d) [22,23], two other methods, namely displacement coefficient method [24] and capacity spectrum method [25,26], have also been proposed. Based on the existing literature review, so far, no study has investigated the accuracy of these methods in estimating the performance point of tunnel-form concrete system, and so the efficiency and sufficiency of these methods in this context remain unclear. Furthermore, the value of the effective damping ratio in the system (β_e) and its role in increasing the prediction accuracy of the methods are still unclear. Based on the provided explanations, the main research questions are as follows:

1. What is the effective damping ratio in the tunnel-form system?
2. How accurate is the displacement coefficient method in estimating the target displacement (or performance point) of tunnel-form buildings? What is the main weakness of this method and how can it be addressed?
3. How accurate is the capacity spectrum method in estimating the performance point (or target displacement) of tunnel-form buildings? What is the weakness of this method and what is the solution to overcome it?
4. To what extent is the method based on using the displacement amplification factor in linear analyses and the code-based approach in assessing the seismic performance of conventional structural systems reliable for the tunnel-form system?
5. What is the appropriate approach for mitigating inherent uncertainties related to future earthquakes in the process of estimating the performance point?

This study aims to address such questions and is organized into seven separate sections. The methodology is presented in Section 2, where the

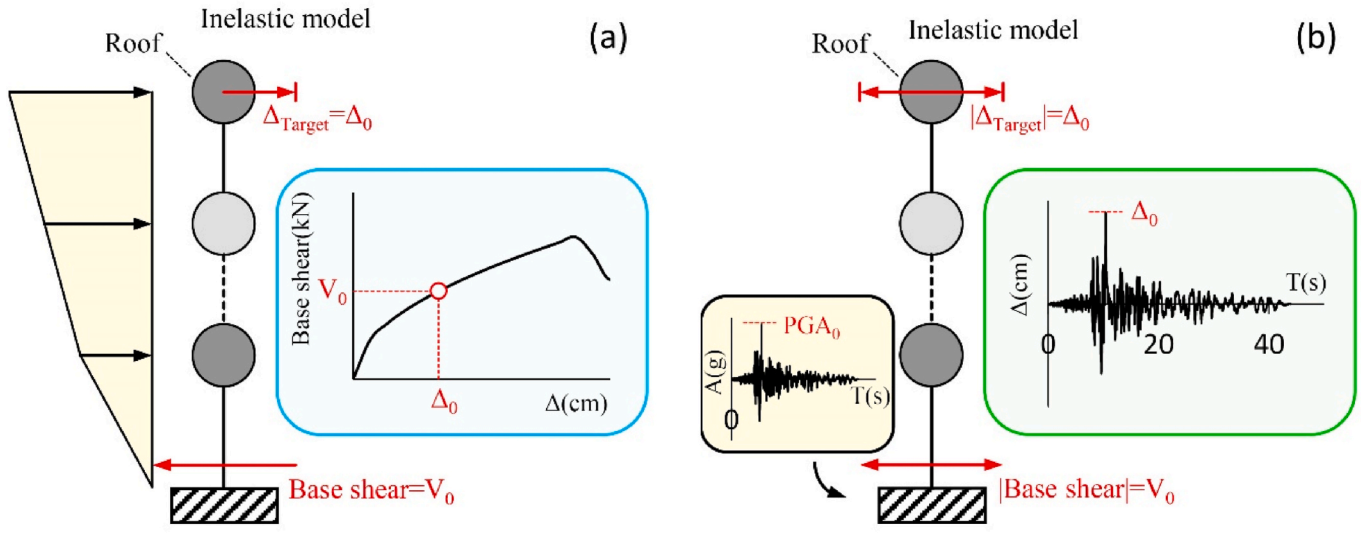

Fig. 2. Interpretation of the performance point in a hypothetical model (a) Pushover analysis (b) Nonlinear time-history analysis.

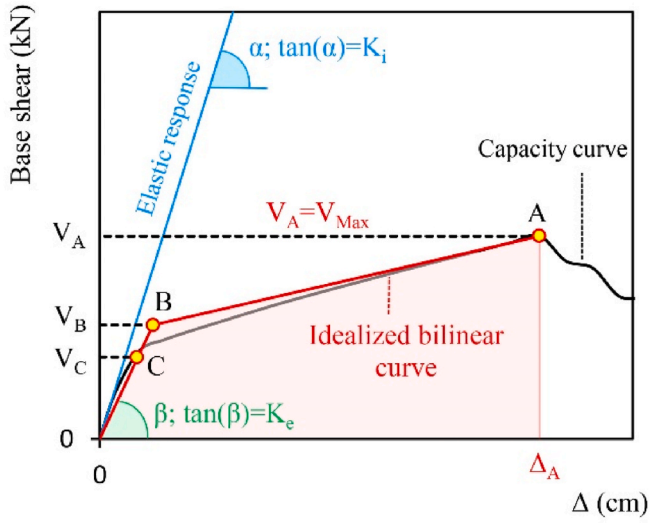

Fig. 3. Smoothing the capacity curve of the model and introduction of the main parameters (schematic).

Table 1
Numerical values for site class factor (a) [20].

Site class	A (1500 ≤V_s)	B (760 ≤V_s < 1500)	C (360 ≤V_s < 760)
a	130	130	90

V_s: Average shear wave velocity (m/s).

Table 2
Values of effective mass factor (C_m) for concrete shear wall systems [20].

No. of stories	Types of lateral system		
	Shear wall	Pier-spandrel	Other
1–2	1.0	1.0	1.0
3 or more	0.8	0.8	1.0

methods for determining the performance point in structures are explained, along with a detailed description of the current study's procedure. In Section 3, the developed numerical models are introduced, followed by an explanation of the nonlinear modeling process and the determination of resistance and deformation parameters of structural elements. Section 4 pertains to structural analysis, where the adopted assumptions are described, and the models are analyzed using time-history and pushover methods.

In Section 5, the adequacy of existing methods for estimating the performance point of tunnel-form buildings under design basis earthquakes is examined. In this section, the weaknesses of each method are identified, and solutions are proposed to address them. Section 6 introduces a new concept called the "probable performance interval". The advantages of using this concept are discussed, and it is suggested as a suitable substitute for the "performance point" parameter. Finally, in Section 7, the main results of the study are presented.

2. Methodology

In nonlinear static analysis (or pushover method), the earthquake lateral load is applied to the structure statically and incrementally according to a specific lateral load pattern (Fig. 2(a)). The primary output of this analysis is the capacity curve of the structure, which is defined as

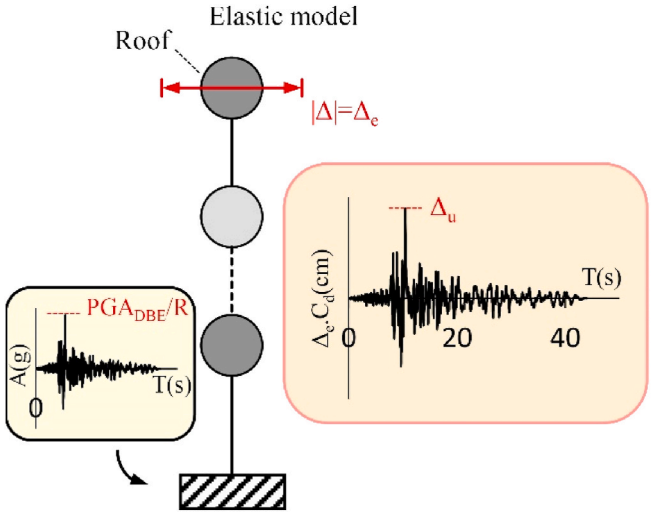

Fig. 5. Linear time-history analysis of a hypothetical model and determination of the target displacement using the displacement amplification factor method.

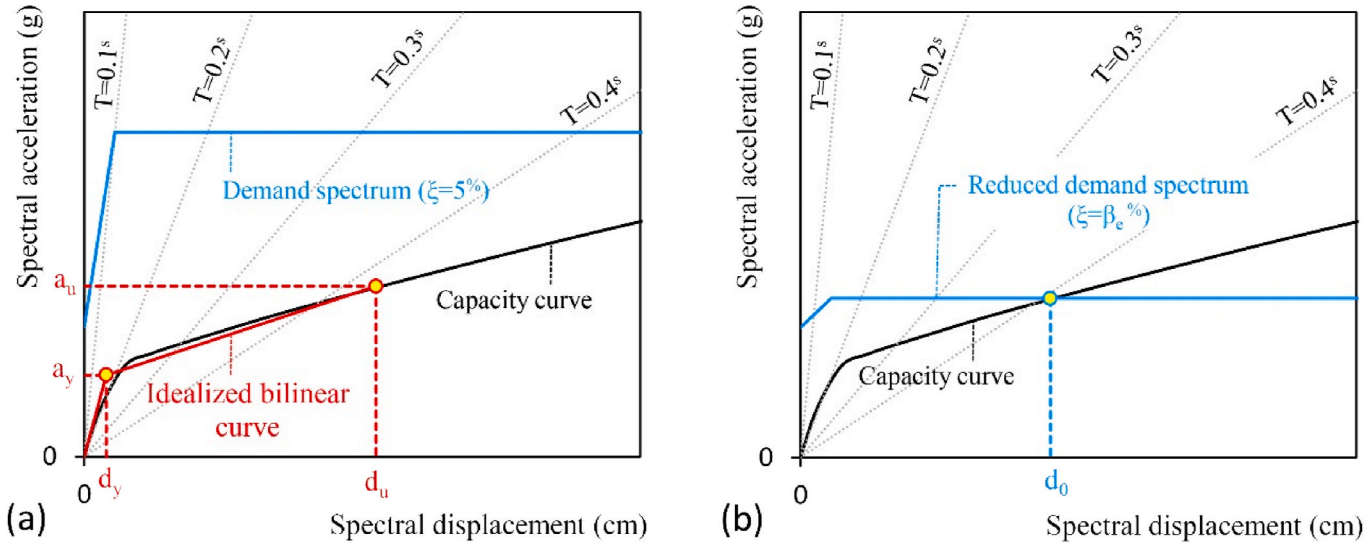

Fig. 4. Introduction of ADRS System (a) Comparison of the structural capacity spectrum with the elastic design spectrum (b) Comparison of the structural capacity spectrum with the reduced demand spectrum.

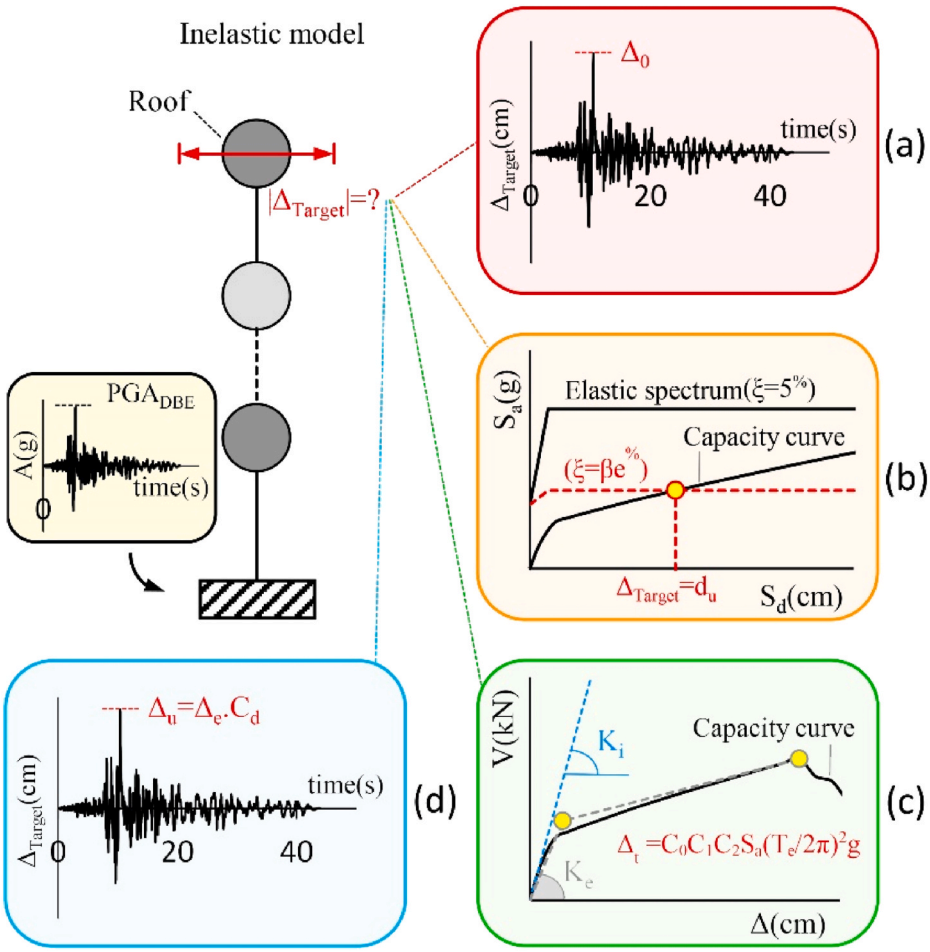

Fig. 6. Determining the target displacement in a hypothetical model with different scenarios (a) Nonlinear time-history analysis (b) Capacity spectrum method (c) Displacement coefficient method (d) Displacement amplification factor method.

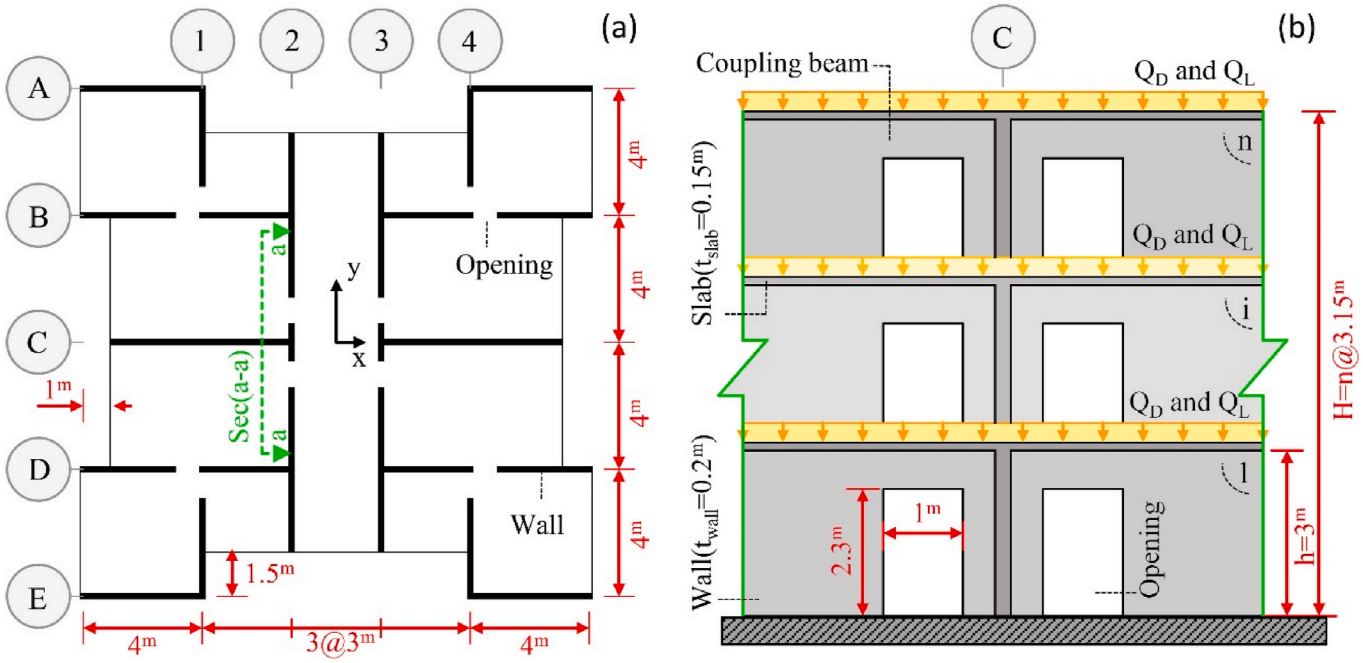

Fig. 7. Studied tunnel-form buildings (a) Typical floor plan (b) Cross-section view "a-a" in a hypothetical n-story model.

Table 3
Values of dead and live loads for stories and roof (kN/m^2).

Loads	Storey level	
	Stories 1 to n-1	Storey n (Roof)
Q_D	6.4	6.4
Q_L	2.0	1.5

the relation between base shear and the lateral displacement of the control point (usually center of mass at the roof level). On this curve, each displacement on the horizontal axis corresponds to an earthquake of a specific intensity. As shown in Fig. 2(a), for an earthquake with the peak ground acceleration of PGA_0 which corresponds to the displacement of Δ_0 , it is expected that, when the structure is analyzed under the mentioned earthquake, the maximum displacement of the control point will be close to Δ_0 (see Fig. 2(b)). In other words, if the selected lateral load distribution pattern is appropriate and close to reality, by pushing the structure up to Δ_0 , it is expected that the deformations and internal forces of the members will be close to the state when the structure is subjected to an earthquake with the mentioned intensity (PGA_0) under nonlinear time-history analysis.

It can be observed that in the process of assessing the seismic performance of structures under a desired hazard level using pushover analysis, the performance point corresponding to that hazard level is a crucial parameter. In fact, during pushover analysis, it is necessary to determine and evaluate the deformations and internal forces of the members at the target displacement [24]. According to existing standards, the performance point (or target displacement) can be estimated using three methods: The Displacement Coefficient Method, the capacity Spectrum Method, and the Displacement Amplification Factor Method.

In the following subsections, each method will be introduced, and the procedure of the current study will be explained.

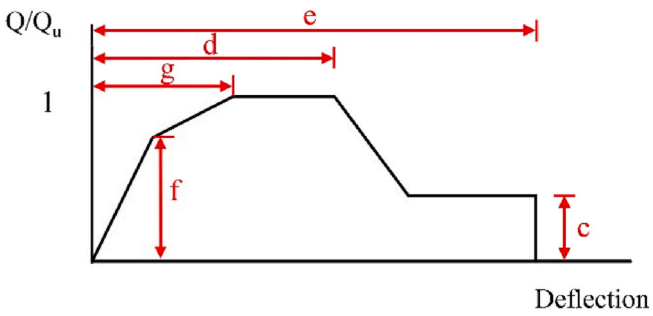

Fig. 9. Generalized Force-Deformation relation concrete elements or components [24].

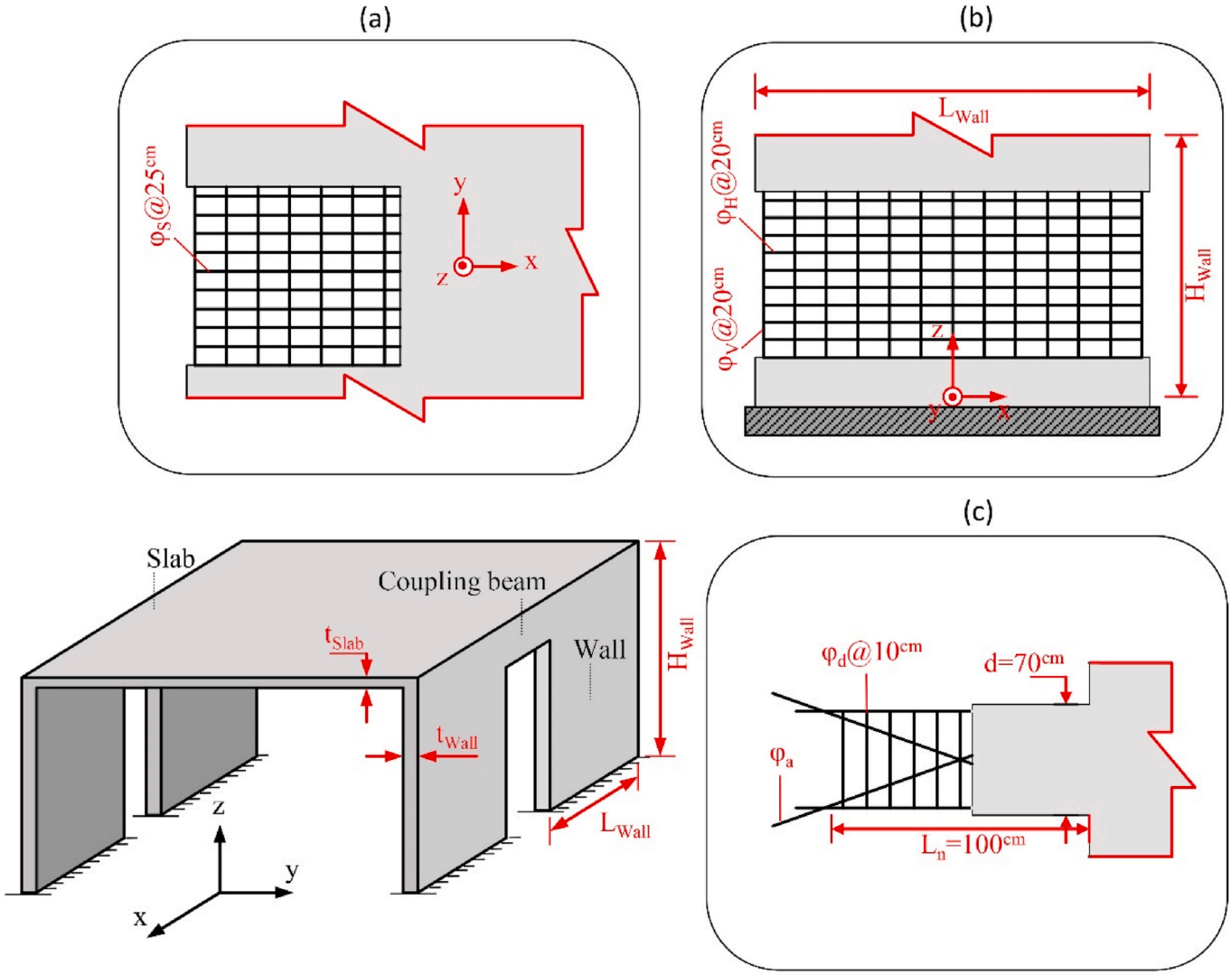

Fig. 8. Reinforcement details of structural elements (a) Slabs (b) Walls (c) Coupling beams.

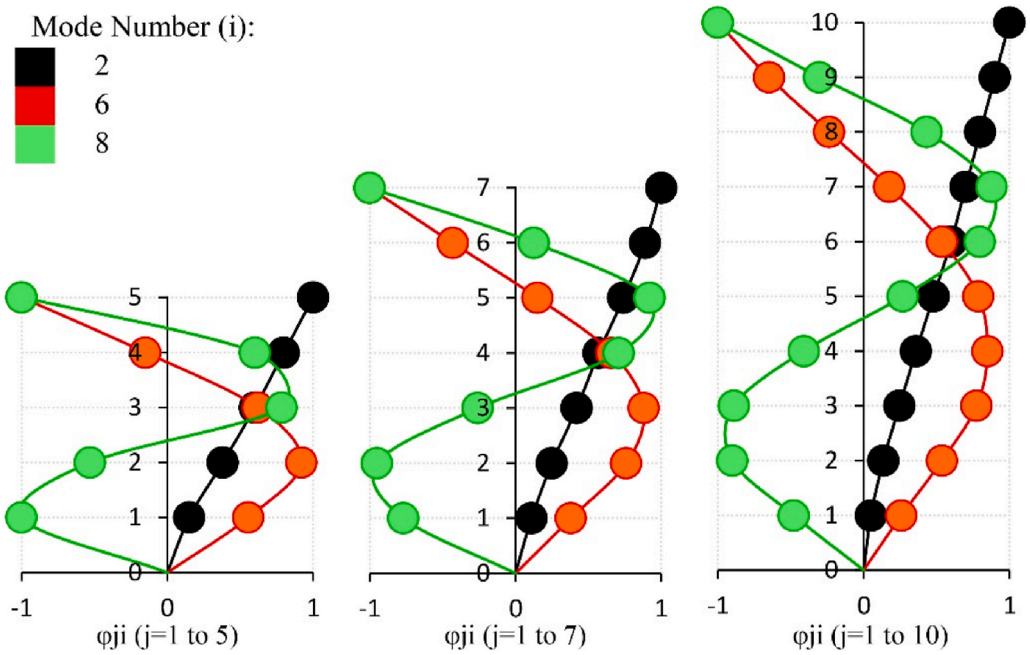

Fig. 10. Mode shapes in the principal direction (*y*) up to 90 % mass participation (a) 5-story building (b) 7-story building (c) 10-story building.

Table 4
Mode properties including time period (T) and effective mass factor (M) in the principal direction of plan (*y*) up to 90 % mass participation.

Mode no.	5-Storey building		7-Storey building		10-Storey building	
	T(sec)	M(%)	T(sec)	M(%)	T(sec)	M(%)
2	0.139	79.60	0.240	77.52	0.445	75.41
6	0.036	14.18	0.061	14.32	0.095	14.47
8	0.023	4.38	0.032	4.52	0.049	4.73

2.1. Displacement coefficient method

In this approximate method, the target displacement of the structure (Δ_t) is obtained from Equation (1) [24]. The prerequisite for using this equation is to smooth the capacity curve of the structure and replace it with a simpler bilinear curve (see Fig. 3). According to Equation (1), in this method, the target displacement of the structure is obtained by modifying the displacement of the elastic single-degree-of-freedom system.

As seen in Fig. 3, the process of smoothing the capacity curve includes determining three key points. Point *A* is considered the target and corresponds to the maximum shear capacity in the system ($V_A = V_{Max}$). Point *B* corresponds to the effective yield base shear of the structure ($V_B = V_y$). This point is selected so that its corresponding shear force is always less than the maximum shear capacity of the system ($V_y < V_{Max}$). Additionally, with the condition that the intersection of the initial slope of the developed bilinear curve with the capacity curve (Point *C*) corresponds to 60 % of the effective yield base shear of the structure ($V_C = 0.6V_y$). Moreover, up to the displacement corresponding to the target point (Δ_A) should ensure that the area under the original and bilinear curves is equal [24].

$$\Delta_t = C_0.C_1.C_2.Sa\left(\frac{T_e}{2\pi}\right)^2.g \tag{1}$$

$$T_e = T_i\sqrt{K_i/K_e} \tag{2}$$

In Equation (1), the parameter T_e is the effective fundamental period of the building in the direction under consideration (in seconds) and is calculated from Equation (2). In Equation (2), T_i is the elastic fundamental period (in seconds) in the direction under consideration calculated by elastic dynamic analysis. In the latter equation, parameters K_i

Table 5
Main components of the selected original earthquakes for generating artificial records.

Records	Earthquake & Year	Station	R[a](km)	Component	M_w	PGA(g)
R_1	Cape Mendocino (US), 1992	Eureka – Myrtle & West	41.97	90	7.1	0.18
R_2	Cape Mendocino (US), 1992	Loleta Fire Station	25.91	270	7.1	0.26
R_3	Cape Mendocino (US), 1992	Fortuna – Fortuna Blvd	19.95	0	7.1	0.12
R_4	Chi-Chi (Taiwan), 1999	TCU042	26.31	E	7.6	0.25
R_5	Chi-Chi (Taiwan), 1999	TCU070	19.00	E	7.6	0.25
R_6	Chi-Chi (Taiwan), 1999	TCU106	15.00	E	7.6	0.16
R_7	Darfield (New Zealand), 2010	Heathcote Valley Primary School	24.50	E	7.0	0.63
R_8	Iwate (Japan), 2008	Yuzawa Town	25.56	NS	6.9	0.24
R_9	Iwate (Japan), 2008	Tamati Ono	28.90	NS	6.9	0.28
R_{10}	Kern County (US), 1952	Taft Lincoln School	38.42	111	7.4	0.18
R_{11}	Kocaeli (Turkey), 1999	Iznik	30.73	90	7.5	0.13
R_{12}	Landers (US), 1992	Barstow	34.86	90	7.4	0.14
R_{13}	Montenegro(Yugoslavia), 1979	Herceg Novi - O.S.D. Paviviv	23.59	90	7.1	0.26
R_{14}	Northridge (US), 1994	Hollywood – Willoughby Ave	23.07	180	6.7	0.24
R_{15}	Northridge (US), 1994	Big Tujunga, Angeles Nat F	19.74	352	6.7	0.25

R: Closest distance to fault rupture.

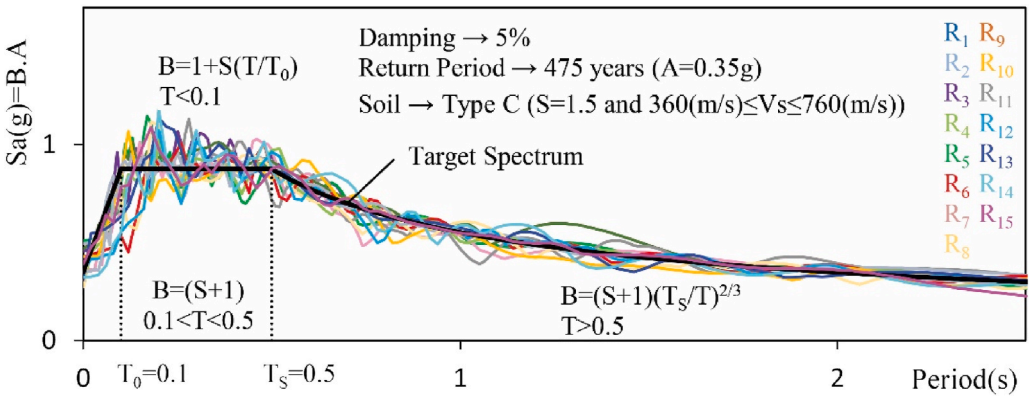

Fig. 11. Comparison of spectral acceleration curves obtained from artificial records with the design spectrum.

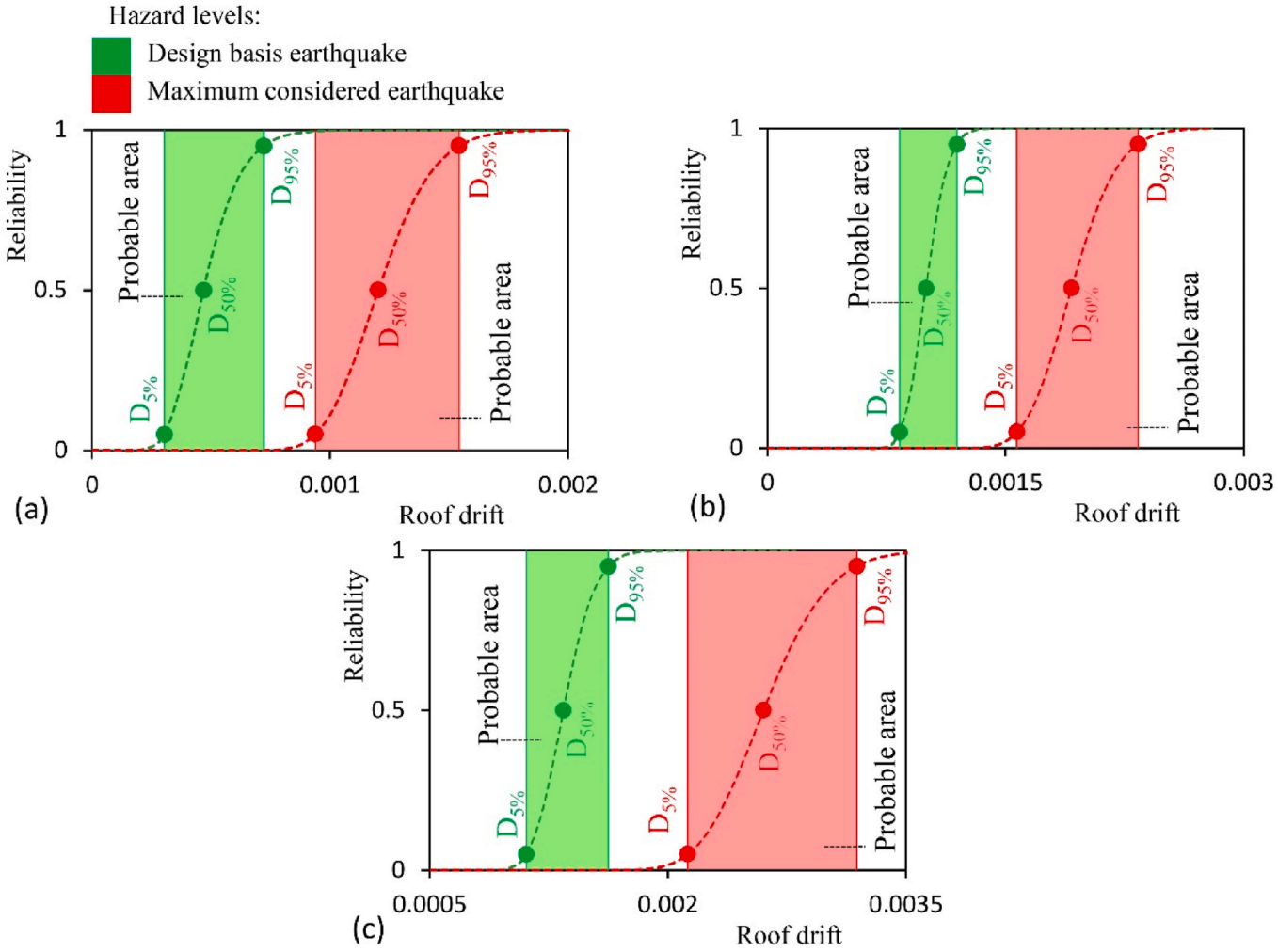

Fig. 12. Probabilistic distribution of maximum roof drift response (target drift) at design basis and maximum considered earthquakes (a) 5-story building (b) 7-story building and (c) 10-story building.

and K_e are the elastic lateral stiffness and effective lateral stiffness in the direction under consideration, respectively (see Fig. 3 again).

In Equation (1), the parameters g and Sa represent the acceleration of gravity and the response spectrum acceleration of the single-degree-of-freedom system at the effective fundamental period and damping ratio of 5 % ($Sa(T_e\&5\%)(g)$), respectively. It is noteworthy that in this study, the value of g is taken as 9.81 m/s. The other parameters of Equation (1) are introduced as follows:

- C_0: modification factor to relate spectral displacement of an equivalent single-degree-of-freedom system to the roof displacement of the building multi-degree-of-freedom system. Depending on the number of stories, type of structural system and lateral load distribution pattern, simplified approximate methods for determining this parameter have been provided [20].
- C_1: modification factor to relate expected maximum inelastic displacements to displacements calculated for linear elastic response.

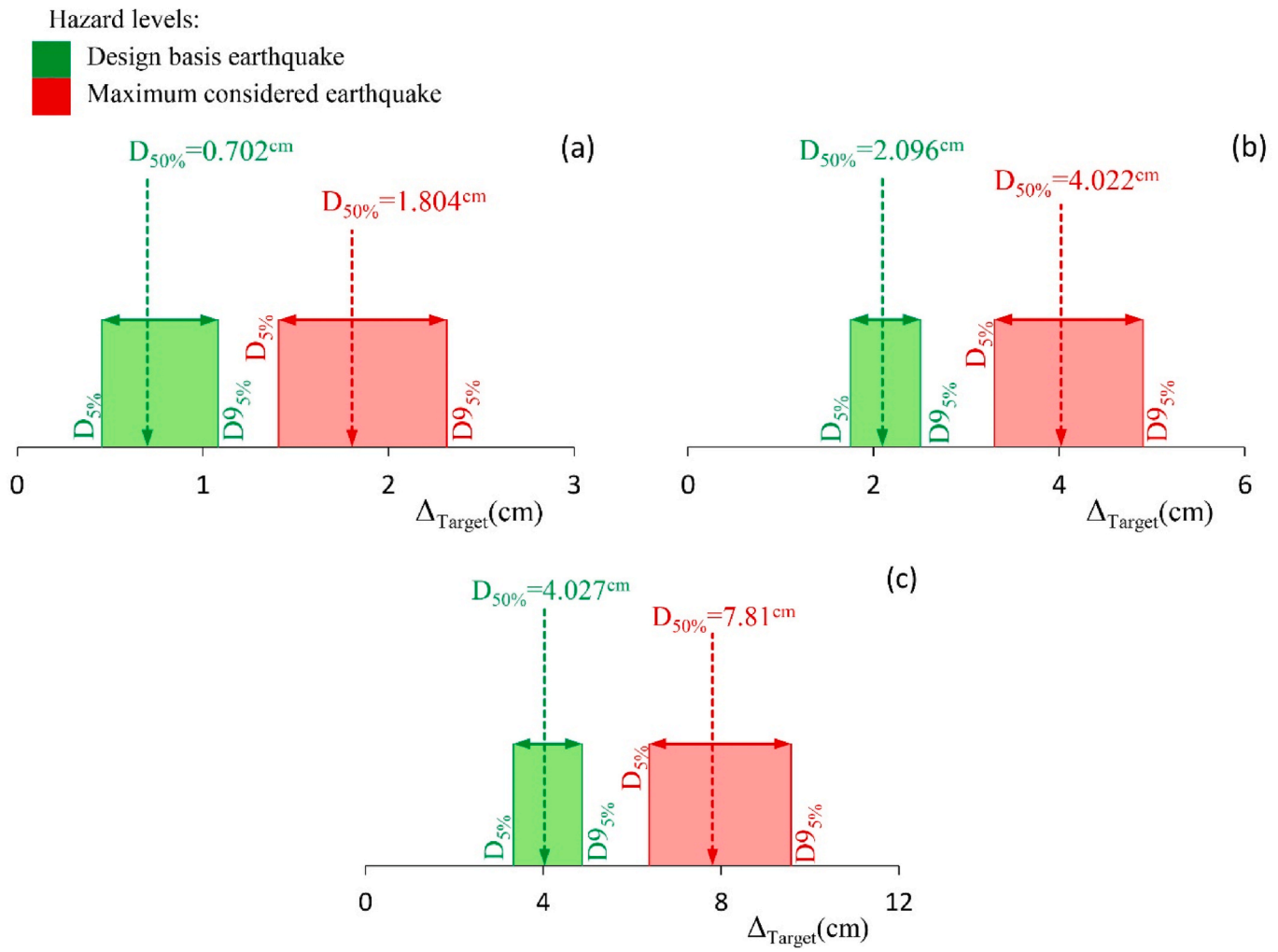

Fig. 13. Probable range of target displacement at design basis and maximum considered earthquakes (a) 5-story building (b) 7-story building and (c) 10-story building.

Depending on the effective period of structure (T_e), this parameter is calculated from Equation (3). In Equation (3), a is site class factor which is selected based on the soil type and shear wave velocity at the site (V_s), as given in Table 1.

$$C_1 = 1 + \frac{\mu_{Strength} - 1}{aT_e^{\,2}} \; for \; 0.2^{sec} < T_e < 1^{sec} \tag{3}$$

- C_2: modification factor to represent the effect of pinched hysteresis shape, cyclic stiffness degradation, and strength deterioration on the maximum displacement response. Depending on the effective period of the system (T_e), this factor can also be calculated from Equation (4).

$$C_2 = 1 + \frac{1}{800}\left(\frac{\mu_{Strength} - 1}{T_e}\right)^2 \; for \; T_e < 0.7^{sec} \tag{4}$$

In Equations (3) and (4), the parameter $\mu_{Strength}$ represents the strength ratio and is calculated in accordance with Equation (5).

$$\mu_{Strength} = \frac{Sa}{(V_y/W)} C_m \tag{5}$$

In Equation (5), the parameter Sa is the response spectrum acceleration corresponding to the effective period of the system (T_e). C_m is the effective mass factor in the fundamental mode, and W is the effective seismic weight of the building. To calculate C_m , eigenvalue analysis results can be used. However, for simplification, depending on type of structural system and number of stories, numerical values for this parameter are also provided (see Table 2).

Based on the provided explanations and with the help of the described equations, the target displacement (or performance point) of a building with a specific structural system can now be calculated under the desired hazard level.

2.2. Capacity spectrum method

In this method, the performance point is calculated from the intersection of the reduced capacity and demand spectrum [25]. Similar to the displacement coefficient method, the first step in this method is to extract the capacity curve of the structure under a realistic lateral load pattern. In the next step, it is necessary to calculate the elastic demand spectrum for the site. Finally, the elastic demand spectrum and the capacity curve are simultaneously plotted on a coordinate system known as *ADRS* (Acceleration-Displacement Response Spectra).

In the first attempt, an arbitrary performance point is selected on the capacity curve (d_u). As a good approximation this point can be the elastic displacement of the structure (the displacement corresponding to the intersection of the tangent slope of the capacity curve at the origin with the elastic demand spectrum).

By considering (d_u) as the target displacement, the capacity spectrum is smoothed. Here, the capacity curve will also be replaced with a

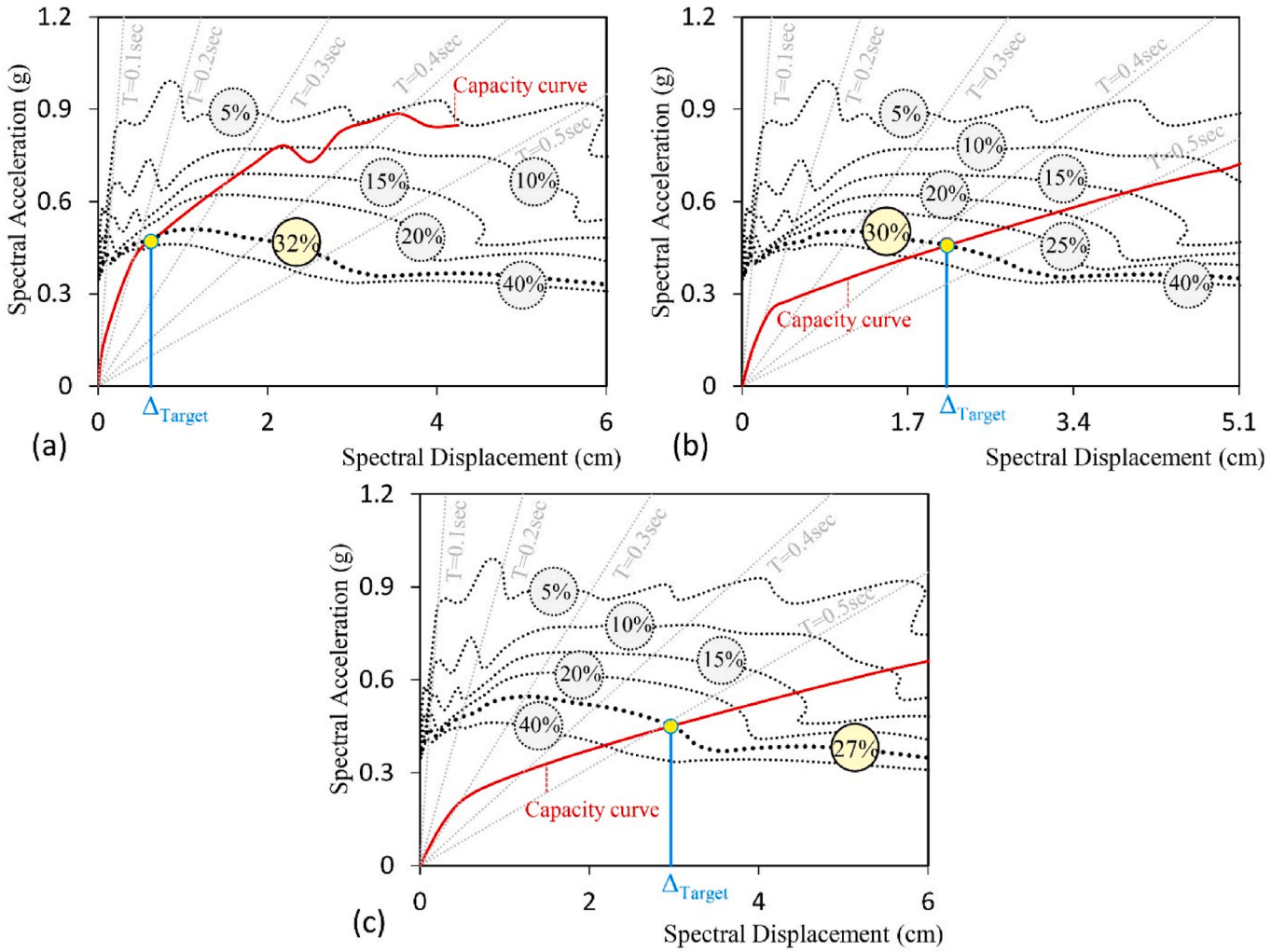

Fig. 14. Determination of effective damping ratio in tunnel-form buildings subjected to artificial ground motion R_2 as the design basis earthquake (a) 5-story building (b) 7-story building and (c) 10-story building.

simplified bilinear curve. The bilinear curve is adjusted such that, firstly, the initial slope is the same as the tangent line to the original curve at the origin, and secondly, the area under the real and bilinear curves up to the performance point (d_u) is approximately equal (see Fig. 4) [26].

Now, the elastic design spectrum must be reduced by a factor dependent on the effective damping ratio (β_e). In this step, nonlinear behavior, stiffness degradation, strength deterioration, and consequently, energy dissipation are included in the calculations up to the displacement corresponding to the performance point (d_u). The spectrum reduction factor (SR) is calculated in accordance with Equation (6) [26].

$$SR_{(\beta_e)} = \frac{5.6 - Ln(\beta_e)}{4} \tag{6}$$

In Equation (6), the parameter β_e represents the effective damping ratio in the structure, which is calculated based on Equation (7). In Equation (7), the parameter β_0 represents the inelastic damping and is calculated from Equation (8). Note that the constant value of 5 in Equation (7) is the inherent elastic viscous damping in the structure [27].

$$\beta_e(\%) = k\beta_0 + 5 \tag{7}$$

$$\beta_0(\%) = \frac{63.7\left(a_y d_u - a_u d_y\right)}{a_u d_u} \tag{8}$$

The parameter k is the damping amplification factor and is a function of the quality of the structural system and the duration of strong earthquake motions. For type A buildings, which are high-quality buildings designed according to seismic codes (complete hysteresis loops without pinching) as classified by ATC-40 [25], this factor is calculated based on the value of β_0 from Equation (9) or (10). As shown in Fig. 4(a), all parameters used in Equations (8) and (9) (i.e., d_u, d_y, a_u, and a_y) are clearly defined and can be easily extracted during the bilinearization of the structural capacity spectrum.

$$k = 1.13 - \frac{0.51\left(a_y d_u - a_u d_y\right)}{a_u d_u} \; for \; \beta_0 > 16.25^{\%} \tag{9}$$

$$k = 1 \; for \; \beta_0 \le 16.25^{\%} \tag{10}$$

Now, by applying the spectrum reduction factor (SR) to the elastic demand spectrum, the reduced demand spectrum is calculated and compared with the structural capacity spectrum (see Fig. 4(b)). The intersection point of the reduced demand spectrum and the capacity curve is determined as the new performance point (d_0). If the difference between the new performance point and the initial value is less than 5 % ($0.95d_u \le d_0 \le 1.05d_u$), the initial value ($d_u$) can be considered the final performance point. Otherwise, it is clear that the new point (d_0) will be used as the new trial, and the calculations will be repeated based on the new point (d_0) according to Equations (8) and (9). It should be noted

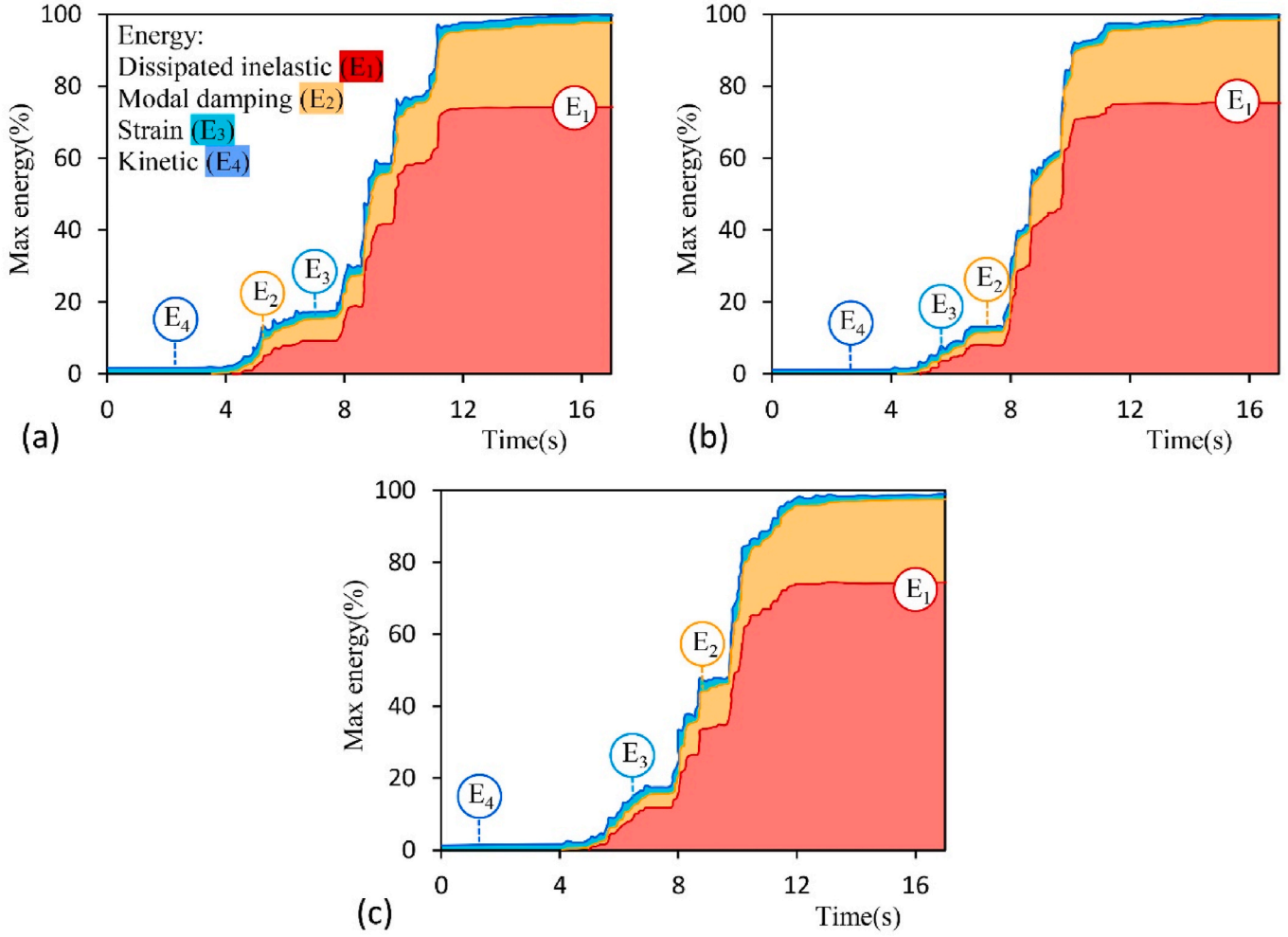

Fig. 15. Energy balance curve under record R_2 as the design basis earthquake (a) 5-story building (b) 7-story building and (c) 10-story building.

that the 5 % error margin is entirely suggested and can vary depending on the required accuracy.

Based on the described scenario and using the available Equations, this method can also be used to calculate the target displacement of a building with a specific structural system under a desired hazard level.

2.3. Method based on displacement amplification factor

This method, well-known among engineers, is carried out using equivalent static analysis or linear time-history analysis. However, the process involves the nonlinear demand spectrum of the site [22,23]. According to study conducted by Mohsenian et al. [17], the equivalent static method does not result in an appropriate estimate of the height-wise distribution of lateral forces in tunnel-form concrete system. So, in the present study, the linear time-history analysis method was used to estimate the performance point using the displacement amplification factor method.

As shown in Fig. 5, the model with linear behavior is analyzed under divided earthquake records by the system's response modification factor (R), and the displacement of the control point (mass center at the roof level) is recorded (Δ_e). Here, the response modification factor reduces the elastic demand spectrum and generates the nonlinear demand spectrum of the site [22,23].

Since the analysis is within the linear behavior range, the recorded responses are multiplied by the system's displacement amplification factor (C_d) to consider nonlinear behavior effects. The product is the desired outcome, called the target displacement ($\Delta_u = C_d\Delta_e$). In seismic design codes, displacement amplification factors are proposed separately based on the material type and the lateral load-resisting system.

If the demand spectrum and parameters R and C_d are specified, the target displacement of a building can also be easily calculated using this method.

2.4. Study procedure

This study aims to evaluate the efficiency and adequacy of methods based on displacement amplification factor, displacement coefficients, and capacity spectrum in estimating the performance point of concrete tunnel-form buildings under the Design Basis Earthquake (*DBE* with $PGA_{DBE} = 0.35g$).

Nonlinear time-history analysis of the models under earthquake records matching the site demand spectrum was performed to determine the probable range of responses, and the median peak displacement of the roof mass center was considered as the accurate response (deterministic performance point) (see Fig. 6 (a)). At this stage, using reverse engineering of the capacity spectrum method, the effective damping ratio of the system (β_e) was also determined using a multi-level approach.

Under the mentioned hazard level (*DBE*), the performance point was also calculated using the methods described in subsections 2.1, 2.2 and 2.3 and compared with the accurate value obtained from the nonlinear time-history analysis. Subsequently, the error level of each method relative to the accurate method was calculated, and the reliability level of the methods was determined (Fig. 6 (b), (c), and (d)).

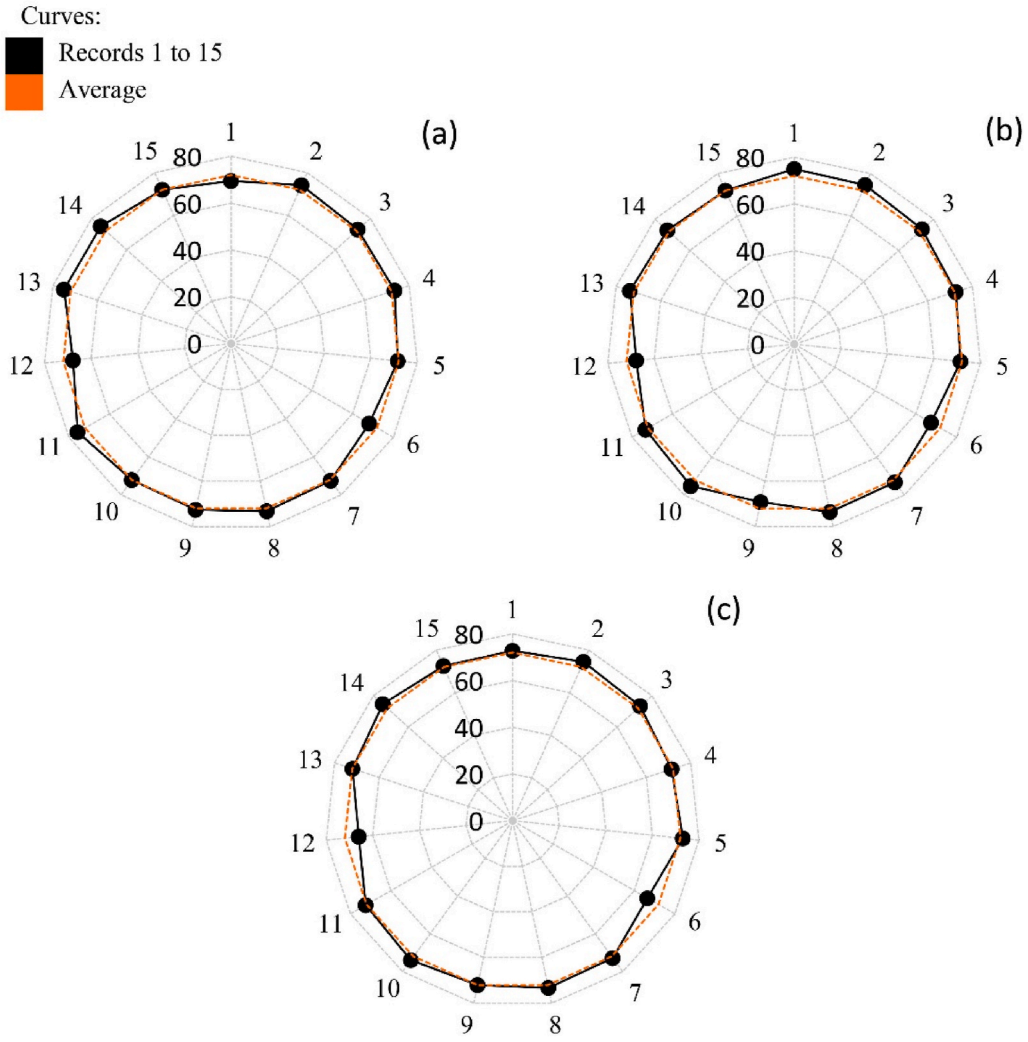

Fig. 16. Percentage of dissipated energy due to nonlinear behaviour of the system under the design basis earthquake (a) 5-story building (b) 7-story building and (c) 10-story building.

Table 6
The 16th, 50th and 84th percentiles for effective damping ratio in studied tunnel-form buildings under design basis earthquake (%).

Percentile(%)	5-Storey building	7-Storey building	10-Storey building
16	25.00	22.82	14.75
50	33.01	28.10	20.00
84	43.21	33.62	22.51

Table 7
Comparison of 16th, 50th and 84th percentiles for effective damping ratio in 7-Story Building between nonlinear time-history analysis and linear interpolation between 5- and 10-Story Models (%).

Percentile(%)	Time-history analysis	Linear interpolation
16	22.82	20.90
50	28.10	27.81
84	33.62	34.89

Finally, by identifying the effective parameters, these methods were refined and improved for more accurate calculation of the target displacement in the concrete tunnel-form system. In this study, to account for the inherent uncertainties related to future earthquakes, the use of a "probable performance interval" instead of a "performance point" was proposed for the first time.

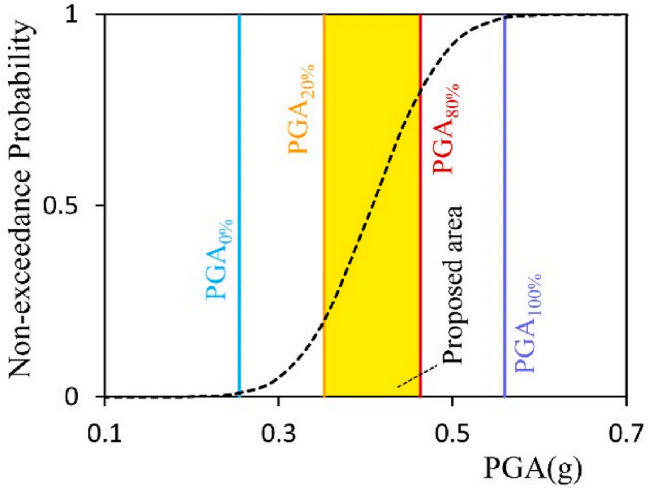

Fig. 17. Probabilistic Distribution of Peak Ground Acceleration (***PGA***) under design basis earthquake.

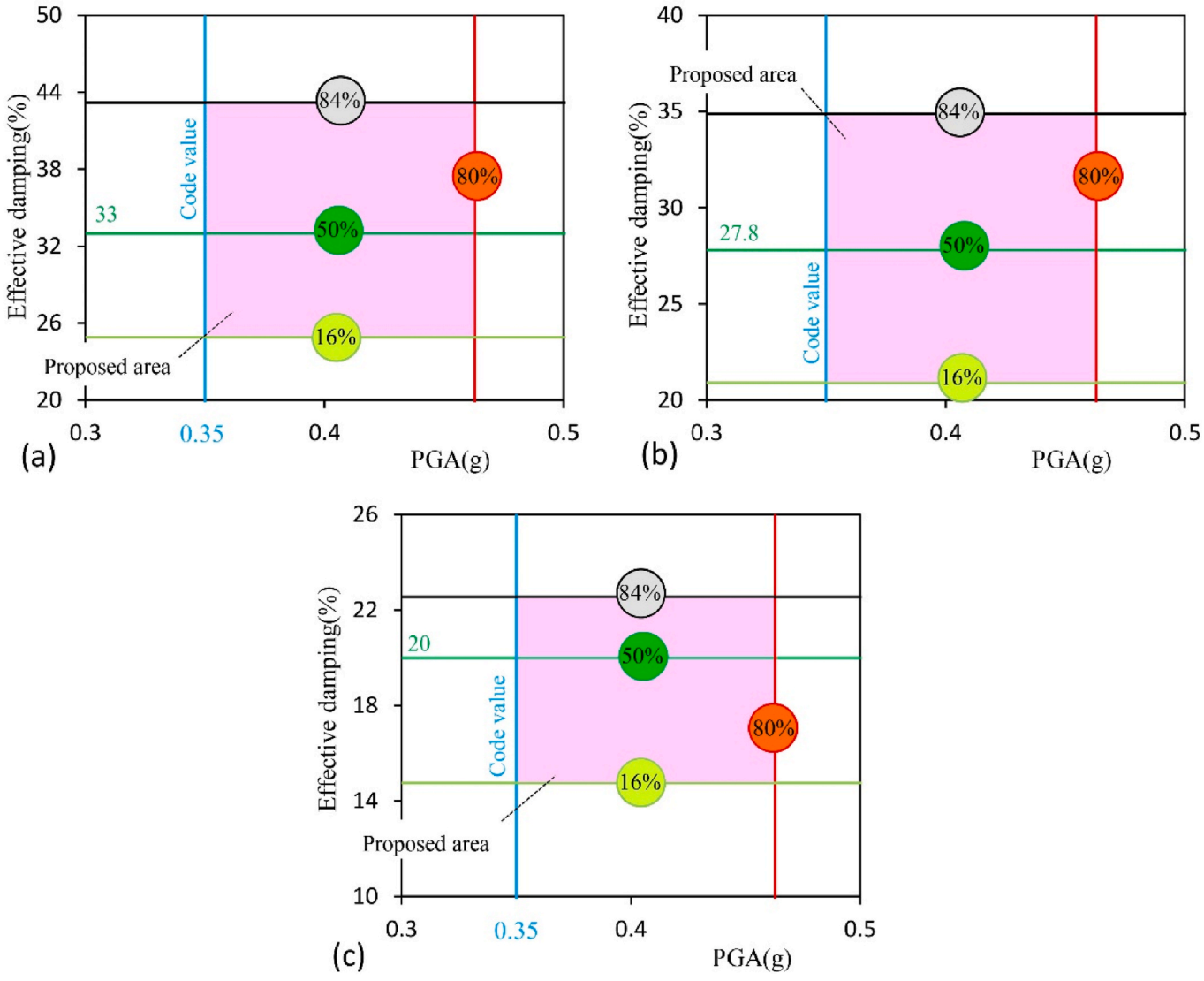

Fig. 18. Multi-level Presentation of effective damping ratio in tunnel-form buildings under design basis earthquake (a) 5-story Building (b) 7-story Building and (c) 10-story Building.

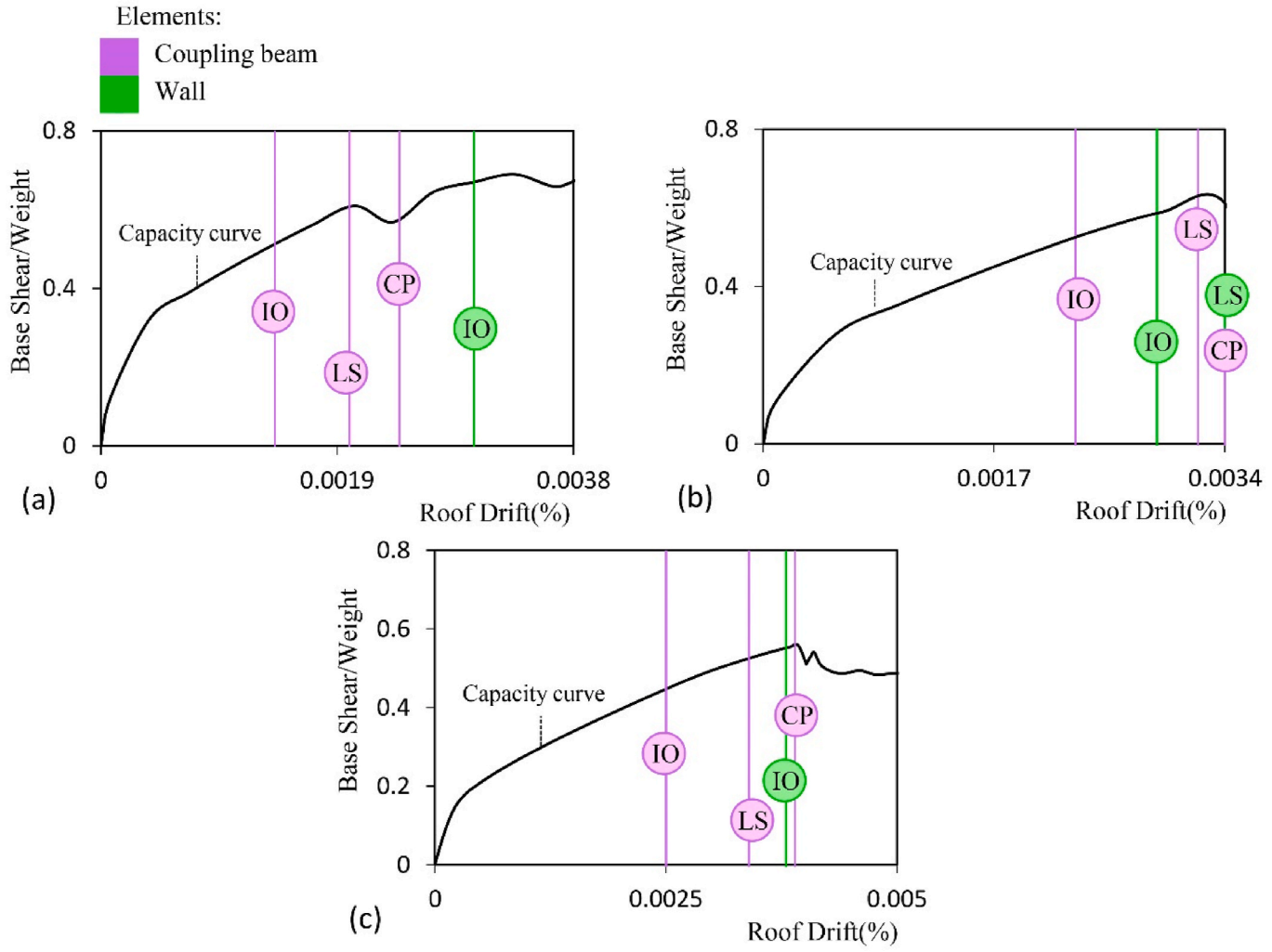

Fig. 19. Capacity curves obtained from pushover analysis (a) 5-story Building (b) 7-story Building and (c) 10-story Building.

Table 8
The control point drifts corresponding to different damage states in structural elements (%).

Performance levels	5-Storey building		7-Storey building		10-Storey building	
	Coupling Beam	wall	Coupling Beam	wall	Coupling Beam	wall
IO	0.14	0.30	0.23	0.29	0.25	0.38
LS	0.20	0.39	0.32	0.34	0.34	0.70
CP	0.24	0.43	0.34	0.36	0.39	0.73

3. Introduction of buildings and description of nonlinear modeling process

For modeling the studied models, the plan depicted in Fig. 7 has been used [28]. The plan belongs to the tunnel-form system and is perfectly symmetric with respect to its principal axes (*x and y*). For the models, the numbers of stories are considered to be equal to 5, 7 and 10 ($n = 5, 7,$ and 10).

The buildings intended for residential use, with a net story height (excluding slab thickness (t_{slab})) of 3 m. Distributed dead (Q_D) and live loads (Q_L) according to Table 3 are considered.

The site has a high seismic potential (return period of 475 years and a design peak acceleration of 0.35*g*), and its soil characteristics align with type C in the ASCE classification (stiff soil with shear wave velocity ranging from 360 to 760 m/s) [23].

The studied buildings were designed according to the Iranian seismic code (Standard 2800) [22] and the American Concrete Institute (ACI) [29], using the ETABS software [30]. In the design process, the yield stress of the rebar (f_y) and the specified compressive strength of the concrete (f_c) were considered equal to 400 and 25 MPa, respectively.

The slab thickness (t_{slab}) was set at 15 cm, reinforced with a two-layer rebar mesh. Each mesh consists of rebars with 8 mm diameter spaced 25 cm apart in both longitudinal and transverse directions (see φ_S in Fig. 8 (a)). The slabs were designed to ensure linear behavior under design basis earthquake.

Wall thickness (t_{wall}) was set at 20 cm to meet the requirement of minimum relative wall area in the plan [5]. Wall reinforcement was also consisting of a two-layer rebar mesh spaced 10 cm apart. Each mesh consists of steel rebars with 8 mm diameter spaced 20 cm apart in both longitudinal (φ_H) and vertical (φ_V) directions (only in the first four stories of the 10-story building, the vertical reinforcement (φ_V) is 12 mm rebars) (Fig. 8(b)).

Architectural criteria and the need for access to internal spaces necessitate inclusion of openings and consequently the formation of coupling beams with length and section height of 1 and 0.7 m, respectively (see Fig. 7 again). In these elements, the ratio of length (L_n) to section height (d) is calculated to be less than 2, ensuring shear failure mode [31,32]. To ensure ductility, seismic closed stirrups and diagonal rebars were considered for reinforcing the coupling beams (see φ_a and φ_d in Fig. 8(c)). Nonlinear modeling and analysis of the buildings were conducted in the PERFORM_3D software environment [33].

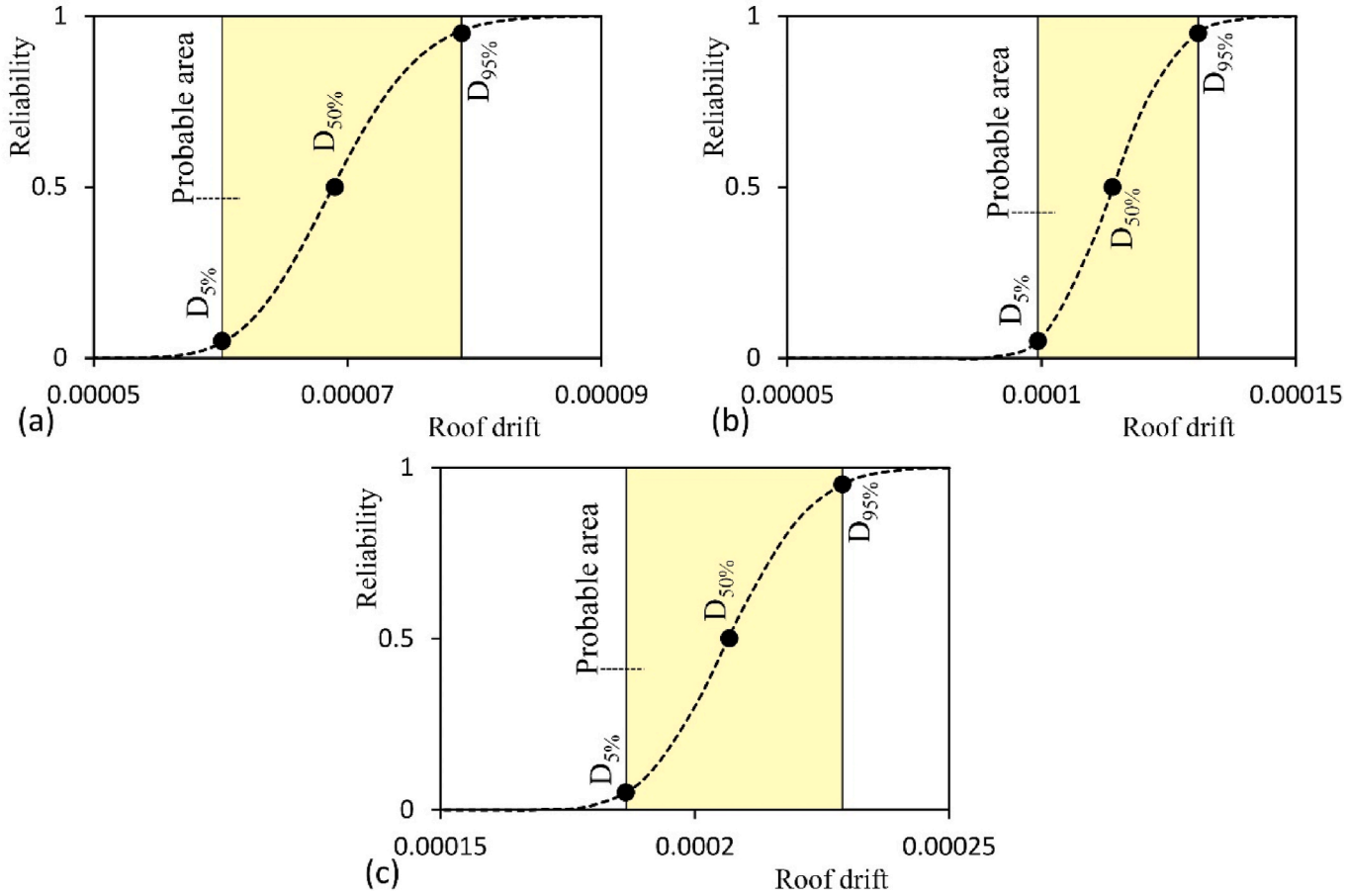

Fig. 20. Probabilistic distribution of maximum roof drift in linear time-history analysis (a) 5-story Building (b) 7-story Building and (c) 10-story Building.

As mentioned, the geometry of the coupling beams leads to shear failure. Based on the study by Mohsenian and Di Sarno [34], the dominant failure mode of the walls in the system is also controlled by shear. Therefore, in modeling the nonlinear behavior of walls and coupling beams, shear demand is considered as the deformation-control parameter. Accordingly, for walls and coupling beams, story drift and chord rotation are considered as the nonlinear response parameters in the analysis [24].

The nonlinear shear behavior curve for the walls and coupling beams is shown in Fig. 9 [24]. In this figure, Q_u represents the nominal shear capacity of the element's section, and for other specified parameters (i.e., f, c, g, d and e), quantitative values are provided separately in the ASCE standard (refer to Table 10–20 in Ref. [24]).

For modeling walls and coupling beams in the PERFORM_3D software, the "shear wall" element was used. Rigid diaphragm, fixed connections, and neglecting soil-structure interaction are other assumptions of this study. Additionally, in the structural analysis process, the gravity load combination (Q_G) is considered according to Equation (11) [24]. In this equation, Q_D and Q_L represent dead and live loads, respectively.

$$Q_G = Q_D + 0.25Q_L \tag{11}$$

Eigenvalue Analysis and the control of wall percentages in both main plan directions (*x and y*) show that stiffness and strength level are lower in the longitudinal direction (*y*). Thus, in this study, the y-direction was selected as the principal direction for analysis (see Fig. 7(a) again). The results of the eigenvalue analysis on buildings up to 90 % modal participation in the principal direction are shown in Fig. 10 and Table 4. It is evident that in Fig. 10, φ_{ji} represents the displacement amplitude of the j^{th} degree of freedom in the i^{th} mode.

Based on the quantitative values in Tables 4 and in all three buildings, the period in the dominant translational mode (mode No. 2) is always less than 1 s, and the effective mass factor is over 75 %. Findings indicate that the dominant lateral load distribution pattern in the buildings is close to triangular [35].

4. Structural analysis and system response

The models introduced in Section 3 were analyzed in the main plan direction (*y*) using nonlinear time-history and pushover analyses. The procedures and assumptions for each analysis are detailed in the following.

4.1. Nonlinear time-history analysis

To better match the selected earthquakes with the site's soil and seismic conditions, artificial records were used. These records were generated by modifying original records in the wavelet domain [36] using Seismomatch software [37].

15 original far-fault earthquakes, consistent with site soil conditions (shear wave velocity between 360 and 760 m/s), were obtained from the PEER database [38]. The primary components of the original earthquakes are listed in Table 5.

As shown in Fig. 11, spectrum and peak ground acceleration of the artificial records align well with the design spectrum.

These records can be considered as the Design Basis Earthquake (*DBE*), and 1.5 times their values can be regarded as the Maximum Considered Earthquake (*MCE*) [37].

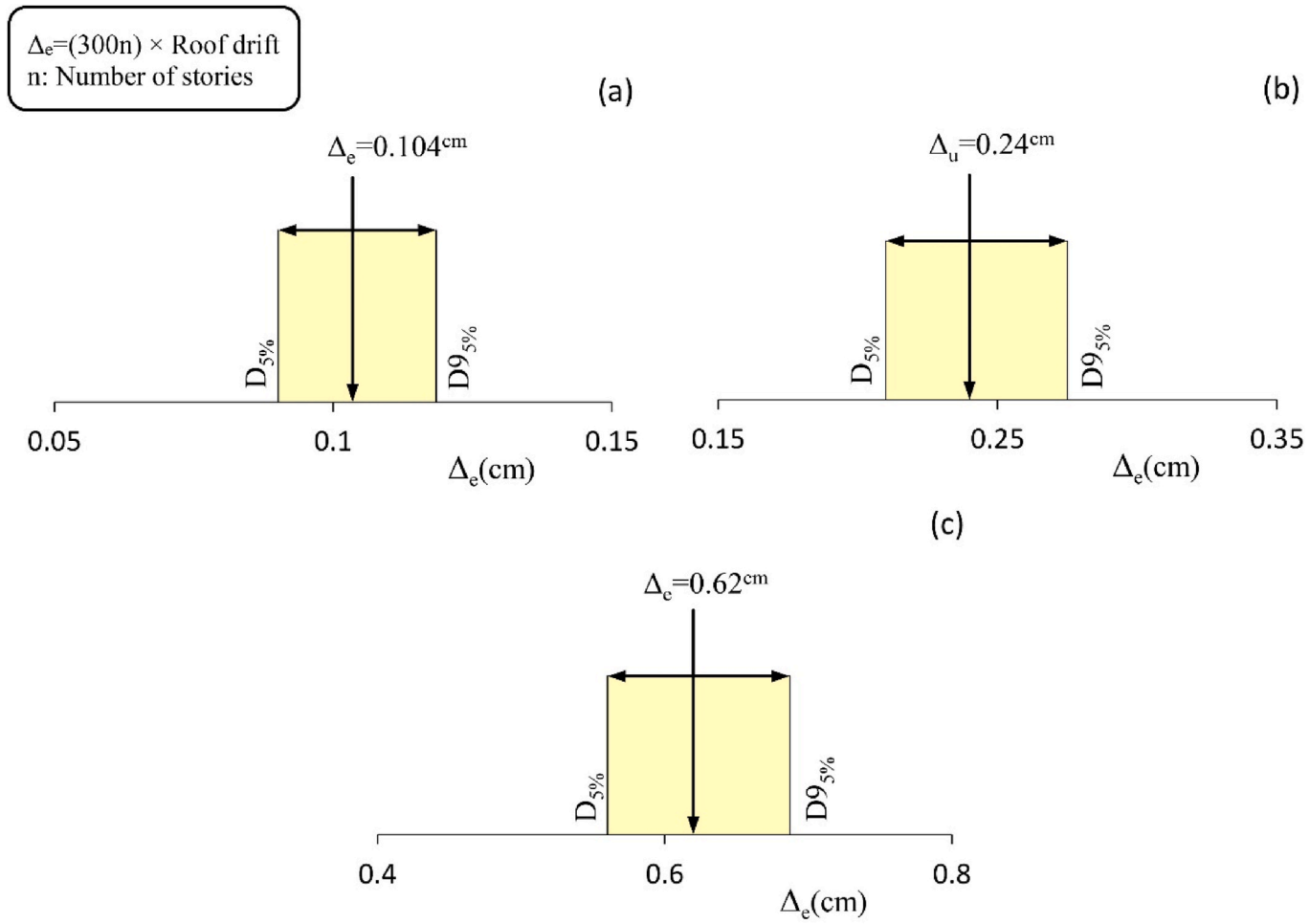

Fig. 21. Probable range of maximum mass center displacement at the roof level in linear time-history analysis (Δ_e) (a) 5-story Building (b) 7-story Building and (c) 10-story Building.

In nonlinear analysis using artificial records, maximum roof displacement was considered as the target displacement. Assuming a log-normal distribution for responses [39], their probabilistic distribution at both hazard levels (*DBE* and *MCE*) was determined [40–42] (see Fig. 12).

Using probabilistic distribution curves, response values corresponding to 5 %, 50 %, and 95 % probabilities ($D_{5\%}, D_{50\%} and D_{95\%}$) can be determined (refer to Fig. 12).

Thus, the probable range of response is specified for each hazard level. As shown in Fig. 13, the target displacement is greater than $D_{5\%}$ and less than $D_{95\%}$ with a 95 % confidence. $D_{50\%}$ is the median and used as a comparison criterion.

At this stage, using the inverse engineering of the capacity spectrum method, the effective damping ratio (β_e) of the system is estimated [26]. According to the explanations in Subsection 2.2, effective damping ratio is calculated to reduce the elastic demand spectrum and determine the target displacement. The target displacement from nonlinear time-history analysis is now available (Δ_{Target}). As shown in Fig. 14, by plotting the capacity spectrum and demand spectrum with various damping levels in the *ADRS* format, the effective damping ratio is determined based on the intersection of the capacity and demand curves at the target displacement.

In Fig. 14, it is observed that under record R_2 as the design basis earthquake, the effective damping in the tunnel-form system exceeds 25 % (32 % for the 5-story building, 30 % for the 7-story building, and 27 % for the 10-story building). These observations are consistent with the findings of Balkaya and Kalkan [3], suggesting that according to ATC-40 classification, the behavior of the tunnel-form system falls under Type A (buildings of excellent quality). In this behavior type, 40 % effective damping ratio in the building is also probable [25].

Since damping is generally associated with the energy dissipation capacity in structures, the absorption and dissipation of energy in buildings at this hazard level should be investigated. To this end, in Fig. 15, an energy balance curve has been extracted for buildings, and the amount of energy dissipated under nonlinear behavior in the system (E_1) has been determined.

Examination of Fig. 15 shows that under record R_2, over 74 % of input energy has been dissipated due to nonlinear behavior of main elements (walls and coupling beams) in system (74.22 % in the 5-story building, 75.54 % in the 7-story building and 74.70 % in the 10-story building). These observations confirm the results obtained from Fig. 14. Under the design basis earthquake, this applies to all artificial records (R_1 to R_{15}) (see Fig. 16).

As observed in Fig. 16, under the design basis earthquake, a significant share of the total input energy into the buildings has been dissipated due to nonlinear behavior in primary elements (walls and coupling beams). Although the dissipated energy varies from one record to another, the average dissipated energy has been estimated at approximately 72 % in all three models (72.34 %, 72.27 % and 72.06 % respectively for the 5-story, 7-story and 10-story buildings).

The process of extracting effective damping ratio (β_e) has been repeated for all artificial records. Since β_e is a function of input motions, this parameter has been extracted for each building across all earthquakes (15 records).

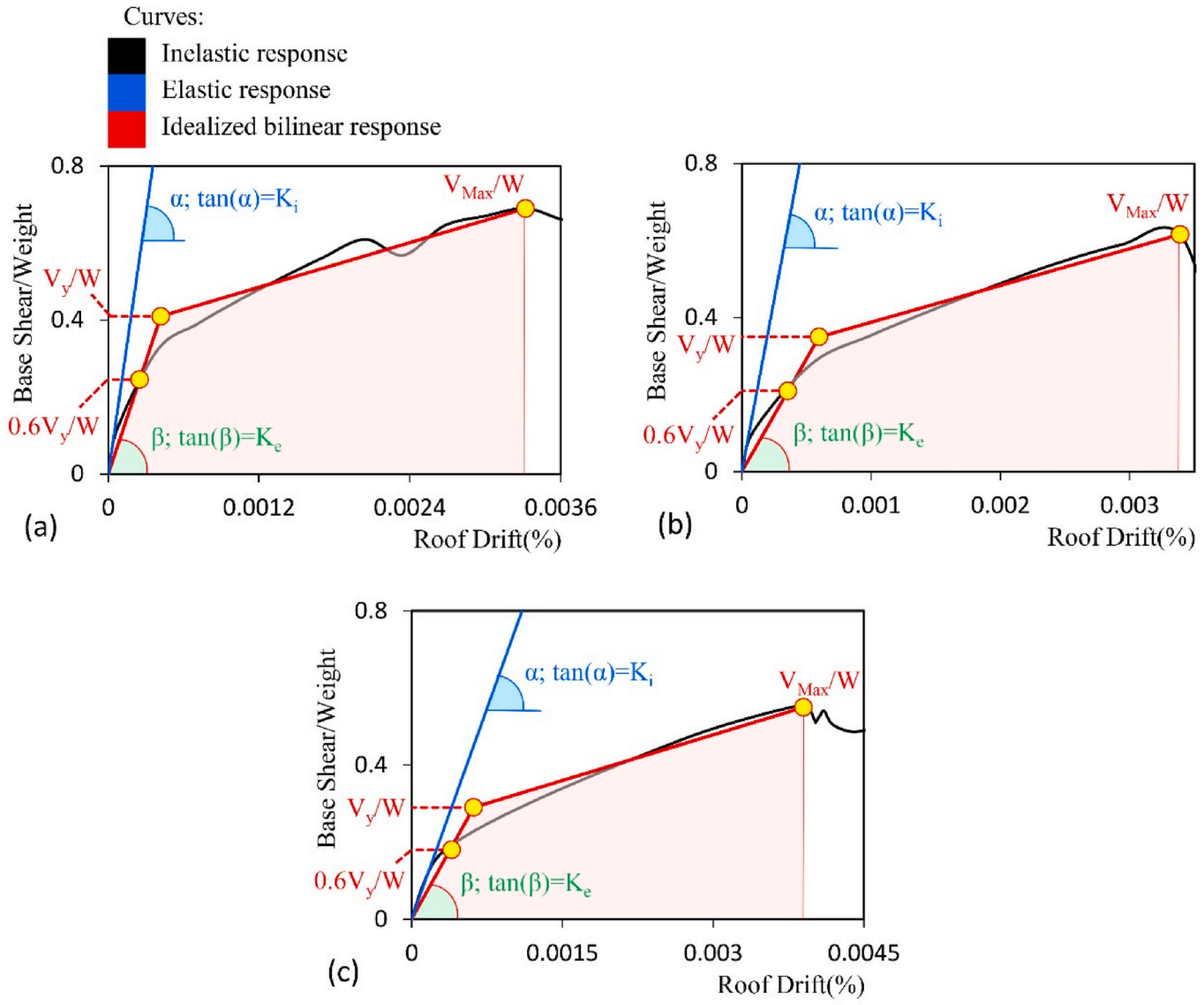

Fig. 22. Comparison of capacity curves with bilinear equivalent curves (a) 5-story Building (b) 7-story Building and (c) 10-story Building.

Table 9
Coefficients calculated in the process of target displacement determination using the displacement coefficient method.

Parameters:	5-Storey building	7-Storey building	10-Storey building
K_i(kgf/cm)	2366070.000	1894899.500	782983.030
K_e(kgf/cm)	1026548.880	624122.300	503571.740
T_i(s)	0.140	0.200	0.445
T_e(s)	0.212	0.348	0.555
Sa(T_e&5 %)(g)	0.875	0.875	0.823
V_y/W	0.410	0.349	0.290
C_m	0.800	0.800	0.800
$R_{Strength}$	1.707	2.000	2.270
C_0	1.300	1.300	1.300
C_1	1.175	1.100	1.046
C_2	1.014	1.010	1.007

Finally, parameters corresponding to the 16th, 50th and 84th percentiles of the statistical population have been determined and categorized for each building (see Table 6).

According to Tables 6 and in each percentile, β_e differs from one model to another and decreases with increasing height (H). When the relationship between effective damping parameters and structural height is linear, interpolation (or extrapolation) between results for the 5- and 10-story buildings will be easily obtained.

Examination of the 7-story building indicates that assuming a linear relationship between parameters β_e and H is sufficiently acceptable (see Table 7). In Tables 7 and it is noted that the difference between linear interpolation and actual values obtained from nonlinear time-history analysis is less than 2 % (1.92 %, 0.3 % and 1.28 % respectively for the 16th, 50th and 84th percentiles).

Based on these results, it appears that effective damping in the tunnel-form system can also be extracted from interpolation (or extrapolation) between available values.

As Stated, β_e varies from one record to another. Therefore, to eliminate inherent uncertainties related to input motions, it is logical to consider a probabilistic variation in the intensity parameter at each hazard level [17]. Accordingly, the maximum acceleration of the generated artificial records (refer again to Fig. 11) is considered as a statistical population with a Log-normal distribution, and the probabilistic distribution of this parameter is extracted (Fig. 17). According to Fig. 17, in this scenario, under design basis earthquake, the parameter *PGA* is certainly greater than 0.25g and less than 0.55g (notice the parameters $PGA_{0\%}$ *and* $PGA_{100\%}$). It is evident from this figure that the proposed acceleration value in the seismic design code for the design

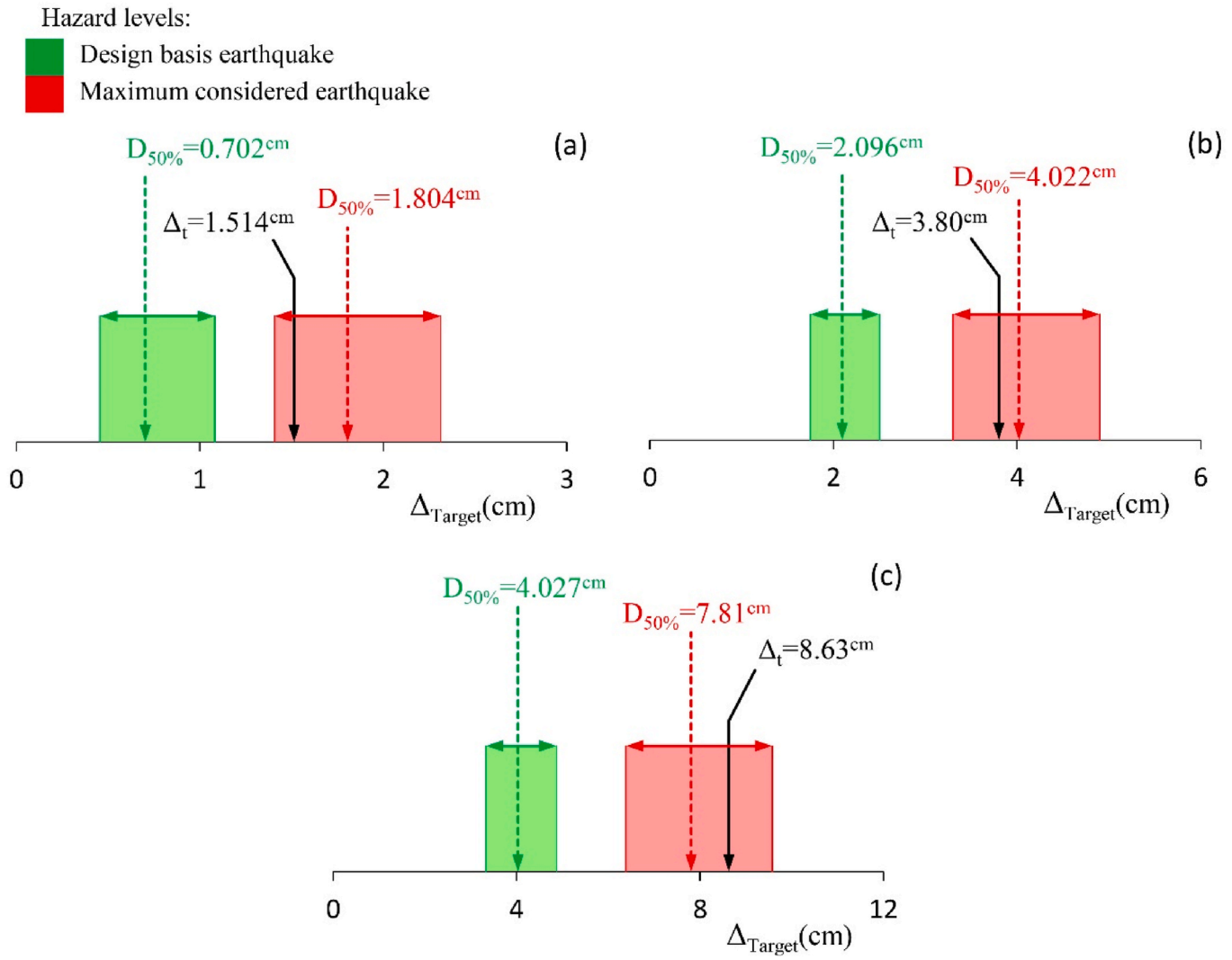

Fig. 23. Comparison of determined performance points by time-history analysis (Δ_{Target}) and displacement coefficient method (Δ_t) (a) 5-story Building (b) 7-story Building and (c) 10-story Building.

basis earthquake (0.35*g*) approximately corresponds to a 20 % probability of non-exceedance ($PGA_{20\%}$). This implies that under design basis earthquake, *PGA* is more likely to exceed 0.35*g* by 80 %.

Finally, by selecting values between $PGA_{20\%}$ and $PGA_{80\%}$ as the most probable area for the parameter *PGA* under the design basis earthquake, effective damping ratio in the system has been proposed in a multi-level approach within the range between the 16th and 84th percentiles (see Fig. 18). As also seen in Fig. 18, under the design basis earthquake, the ranges related to the *PGA* and β_e in the system overlap in a specific region (Proposed area). Considering the direct relationship between acceleration and damping, effective damping ratio (β_e) in the system can be derived from this common region. With this scenario, it is evident that inherent uncertainties related to earthquakes will be reduced to an acceptable level.

4.2. Nonlinear static pushover analysis

The pushover analysis was conducted using the modal method. The modal method combines vibration modes in the direction under consideration with up to 90 % mass participation (refer to Fig. 10). As mentioned earlier, the primary output of this analysis is the capacity curve. For the studied buildings, these curves are depicted in Fig. 19. In these curves, the horizontal axis represents the roof drift (displacement of mass center at roof level divided by the total building height), and the vertical axis represents the base shear normalized by the effective seismic weight of the building.

Furthermore, by examining the local responses of elements during the analysis, the first coupling beams and walls that experience Immediate Occupancy (*IO*), Life Safety (*LS*), and Collapse Prevention (*CP*) performance levels are identified. For each damage state, the corresponding control point drift value has been extracted (see Table 8). Additionally, calculating the performance point of each building under a desired hazard level allows predicting its seismic performance level. It should be noted that the failure criteria and limit states corresponding to different performance levels in the elements have been adopted from the ASCE standard (refer to Table 10–20 in Ref. [24]).

4.3. Linear time-history analysis

The buildings were subjected to linear time-history analysis using artificial records introduced in subsection 4.1 (refer to Fig. 11 again). As explained in subsection 2.3, the model has been analyzed using the inelastic demand spectrum. For this purpose, artificial records have been divided by the system response modification factor. Considering that the aim is to determine the target displacement under the design basis earthquake (475-year return period), a response modification factor of 4 has been used to reduce the elastic demand spectrum [17].

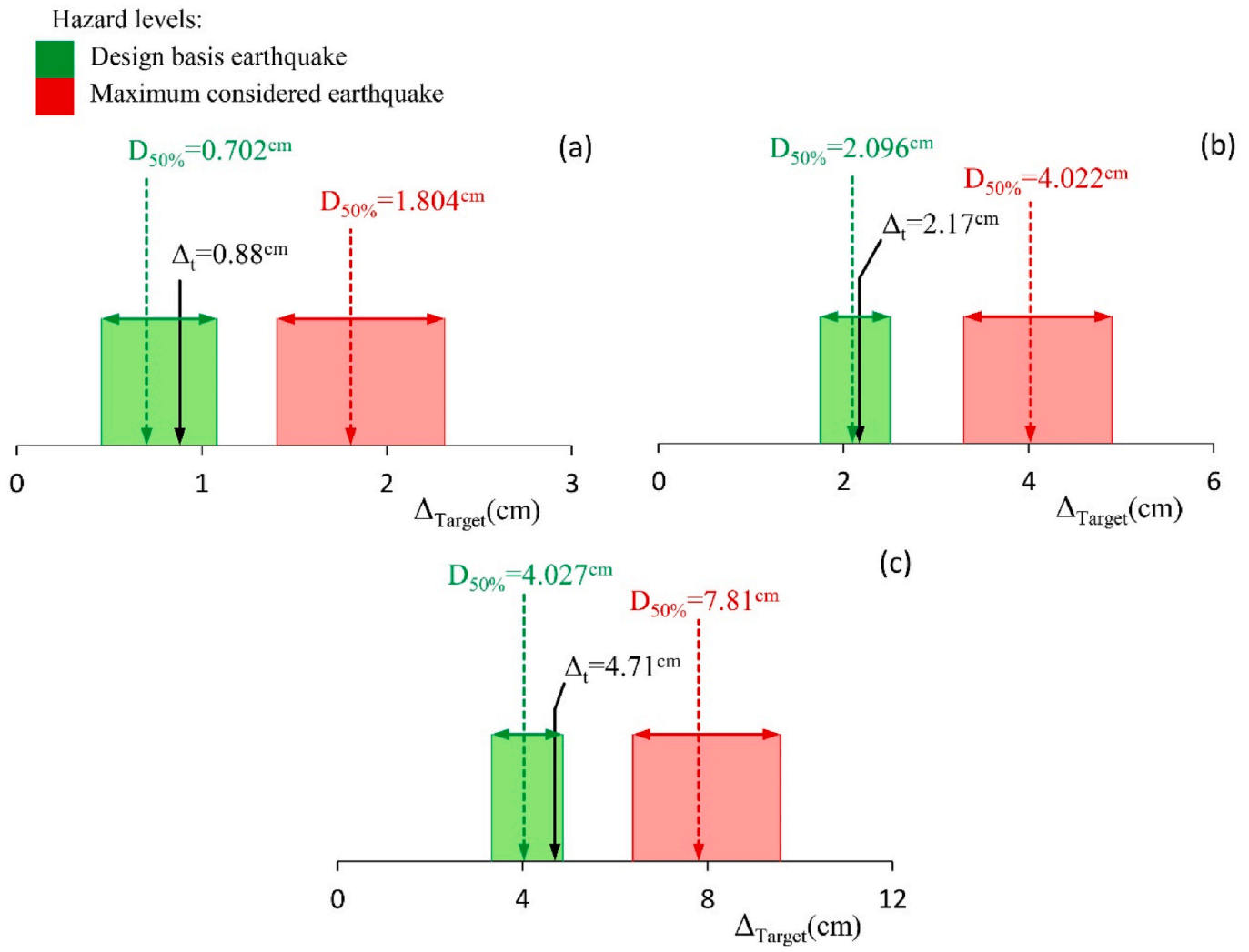

Fig. 24. Determined performance point considering the effective damping in displacement coefficient method (Δ_t) (a) 5-story Building (b) 7-story Building and (c) 10-story Building.

In the following, while analyzing the model, the maximum roof drift has been recorded as the desired response. Using the process outlined in subsection 4.1, here also the probabilistic response has been presented (Fig. 20). Finally, based on the probabilistic distribution curves, the mass center displacement at roof level (Δ_e) corresponding to the probabilities of 5 %, 50 %, and 95 % ($D_{5\%}, D_{50\%} and D_{95\%}$) have been determined and considered as the operation criteria (Fig. 21).

5. Evaluation of the efficiency level of existing methods in assessing the performance point of tunnel-form system

In this section, the results of analyses conducted in Section 4 have been used to estimate the seismic performance point of tunnel-form system under Design Basis Earthquake (*DBE*). As previously mentioned, the results of nonlinear time-history analyses serve as the basis for comparing and evaluating the reliability of other methods (refer again to Fig. 13).

5.1. Displacement coefficient method

To calculate the target displacements using the displacement coefficient method, the capacity curves obtained from the pushover analysis (see Fig. 19) have been adjusted to bilinear form (Fig. 22). Alongside smoothing the capacity curves, all conditions specified in subsection 2.1 have also been applied.

Based on Fig. 22 and using Equations (2)–(5), primary coefficients have been calculated for each model as described in Table 9. Finally, the target displacement of the buildings (Δ_t) under the design basis earthquake have been computed using Equation (1) (see Fig. 23).

According to Fig. 23, for all three buildings, the performance point under *DBE* lies within the response range corresponding to *MCE*. This implies that under *DBE*, the performance point will certainly be less than the estimated values.

Evaluations indicate that the estimation by the displacement coefficient method is inappropriate and highly conservative compared to the median value in accurate nonlinear time-history analysis ($D_{50\%}$). The error of the displacement coefficient method in prediction exceeds 80 % (115.67 % for the 5-story building and 81.29 % and 114.30 % for the 7-story and 10-story buildings, respectively). Based on the obtained results, the displacement coefficient method is deemed inadequate for estimating the performance point of tunnel-form system and is not recommended for use.

In the process of performance point estimation, the spectral acceleration (*Sa*) is a significant parameter (see Equation (1)). Currently, this parameter is derived from elastic demand spectrum (damping = 5 %) at the effective period of structure (T_e) in the direction under consideration

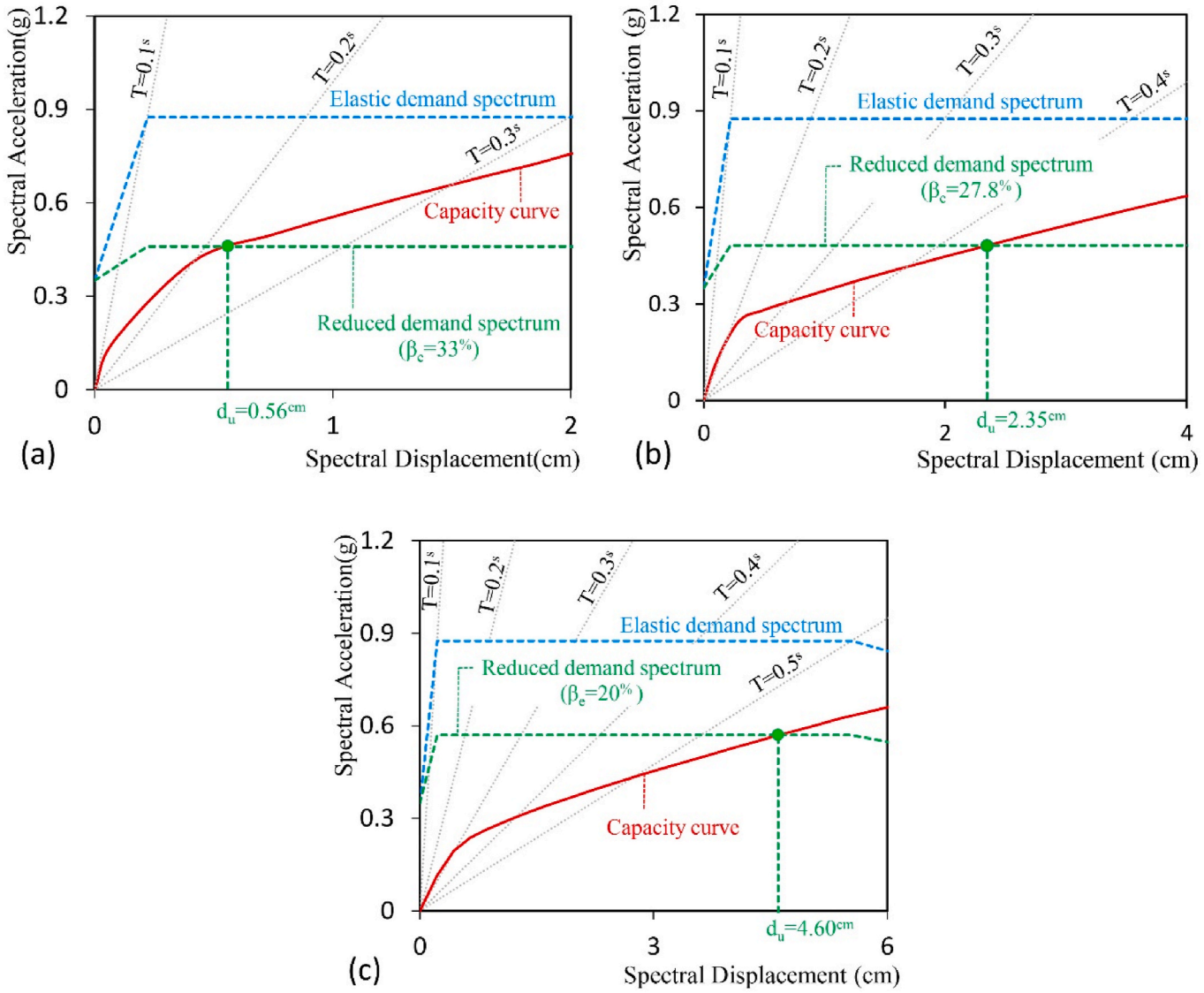

Fig. 25. Determination of performance point using the Capacity Spectrum Method (a) 5-story building (b) 7-story building and (c) 10-story building.

($Sa(T_e\&5\%)(g)$). This is despite the fact that the effective damping in the system is significantly higher than 5 % (refer again to Fig. 18). In the following, while applying the effective damping effect to calculating the spectral acceleration parameter, the accuracy of the displacement coefficient method has been re-evaluated (Fig. 24). In the second series of performance point calculations, the spectral acceleration parameter has been derived from the reduced demand spectrum considering appropriate effective damping ratio ($Sa(T_e\&\beta_e\%)(g)$).

According to Fig. 24, by applying the effective damping effect, the performance point is within the probable response range under the design basis earthquake. In all three models, the prediction error of the method has significantly reduced (25.36 % for the 5-story building, 3.53 % for the 7-story building, and 16.96 % for the 10-story building).

Comparison of Figs. 23 and 24 indicates that with the application of effective damping effects in calculation process, the error of the displacement coefficient method has been reduced by more than 75 % (90.31 % for the 5-story building, 77.76 % for the 7-story building and 97.34 % for the 10-story building). Based on the obtained results, it is strongly recommended that while using the displacement coefficient method, the effects of effective damping ratio should be considered in calculations.

5.2. Capacity spectrum method

According to the explanations provided in section 2.2, the Capacity Spectrum Method is based on trial and error and continues as long as the estimation error remains within permissible margin. In this method, the effects of damping are considered in the calculations [25,26]. Therefore, higher accuracy results are expected compared to the Displacement Coefficient Method. Nevertheless, this method requires more effort. Perhaps “iterations” is one of the main drawbacks of the Capacity Spectrum Method.

The main factor in this method is the effective damping value and consequently the reduction factor of the elastic demand spectrum (see Equations (6) and (7)). Obviously, by defining the effective damping ratio for the lateral resisting system (β_e), the process of determining the performance point becomes independent of trial and error and more cost-effective. This is because Equations (7)–(10) and the calculation steps based on them will no longer be used. In the present study, with the aim of eliminating iterative processes in the Capacity Spectrum Method,

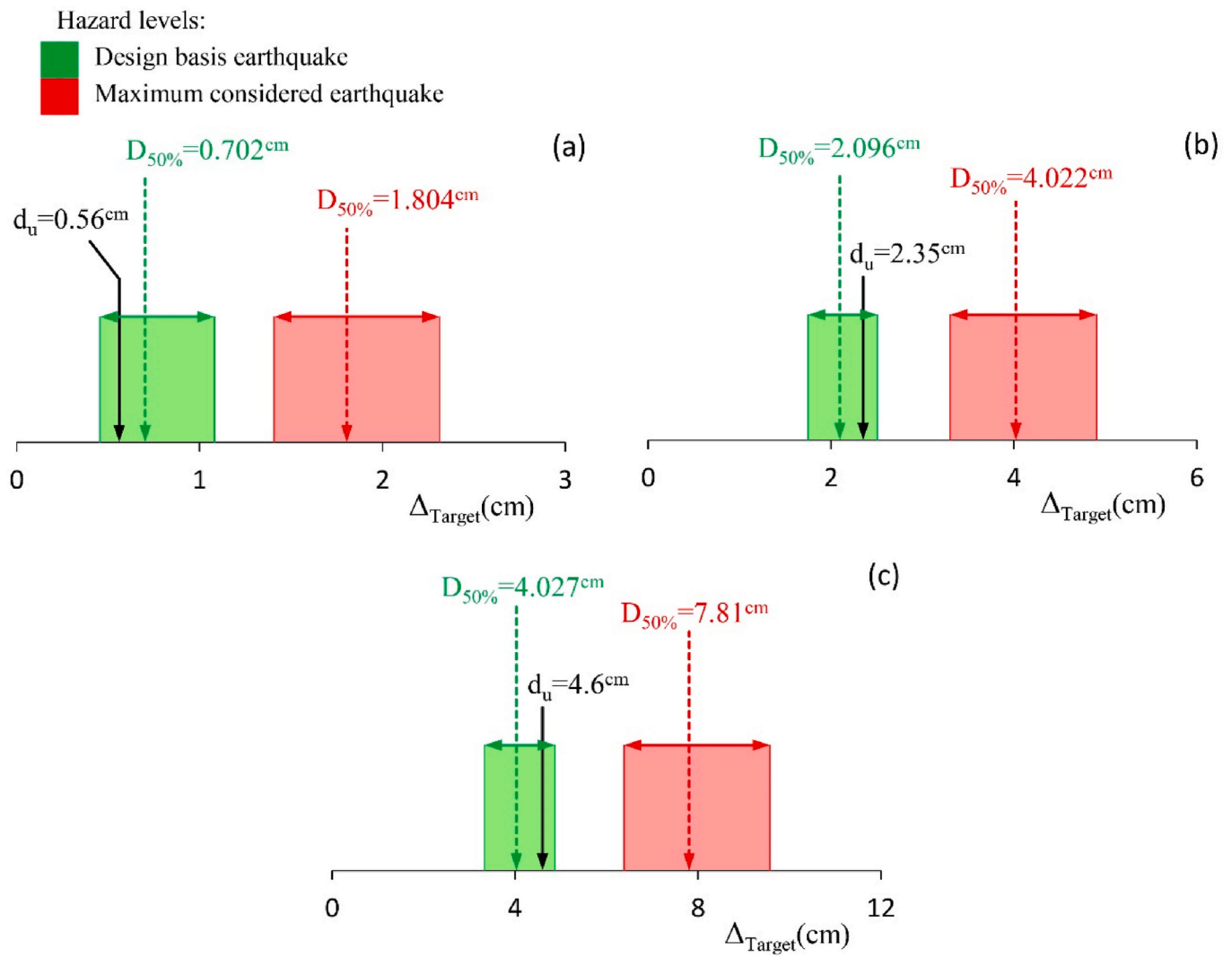

Fig. 26. Comparison of determined performance points by nonlinear time-history analysis (Δ_{Target}) and Capacity Spectrum method (d_u) (a) 5-story building (b) 7-story building and (c) 10-story building.

a multi-level effective damping scheme has been proposed (see Table 6 and Fig. 18).

The capacity curve is determined from the pushover analysis (Fig. 19). Subsequently, by determining damping value corresponding to 50th percentile and using this value in Equation (6), the elastic spectrum reduction factor (*SR*) is determined. According to Fig. 25, after applying the reduction factor, the intersection point of the capacity spectrum and the reduced demand spectrum in the *ADRS* system has been extracted as the performance point.

Examination of Fig. 26 shows that the estimation by the Capacity Spectrum Method has been desirable for determining the performance point of tunnel-form system. In all three buildings, the performance point lies within the appropriate range (probable response range under design basis earthquake). Compared to the median values in the accurate nonlinear time-history analysis ($D_{50\%}$), the prediction error of the performance point by the Capacity Spectrum Method is 20.23 % for the 5-story building and 12.11 % and 14.23 % for the 7- and 10-story buildings respectively. This method does not require the calculation of different coefficients but has provided acceptable results similar to the modified Displacement Coefficient Method (refer again to Fig. 24). It is noteworthy that by using multi-level effective damping, the performance point has been calculated independently of iterative and time-consuming processes just in a single stage. This advantage highlights the Capacity Spectrum Method and prioritizes its use.

5.3. Displacement amplification factor-based method

According to the explanations provided in Subsection 2.3, the accuracy of this simple method depends on the selected amplification factor for the system (C_d). In the available seismic design codes for tunnel-form system, a specific displacement amplification factor has not been provided. The most comparable system with characteristics similar to that is load-bearing wall system. Therefore, similar seismic parameters are used for both systems. In the Iranian seismic design code (Standard 2800) and ASCE, the displacement amplification factor for load-bearing wall system with medium and high ductility levels has been proposed to be 4 and 5, respectively [22,23]. In the present study, a value of 5 has been used as the displacement amplification factor for tunnel-form concrete system.

Finally, according to Fig. 27, the maximum response of the roof displacement from linear time-history analysis under reduced artificial records (see Fig. 21) has been amplified using the selected C_d and subsequently the probable response range under design basis earthquake has been extracted.

In Fig. 27, it can be seen that displacement amplification factor-based method has estimated the response region narrower than the accurate method and often outside the estimated response range (compare green and yellow regions). When compared to the median values ($D_{50\%}$ *and* Δ_u), the error of this method for predicting the performance

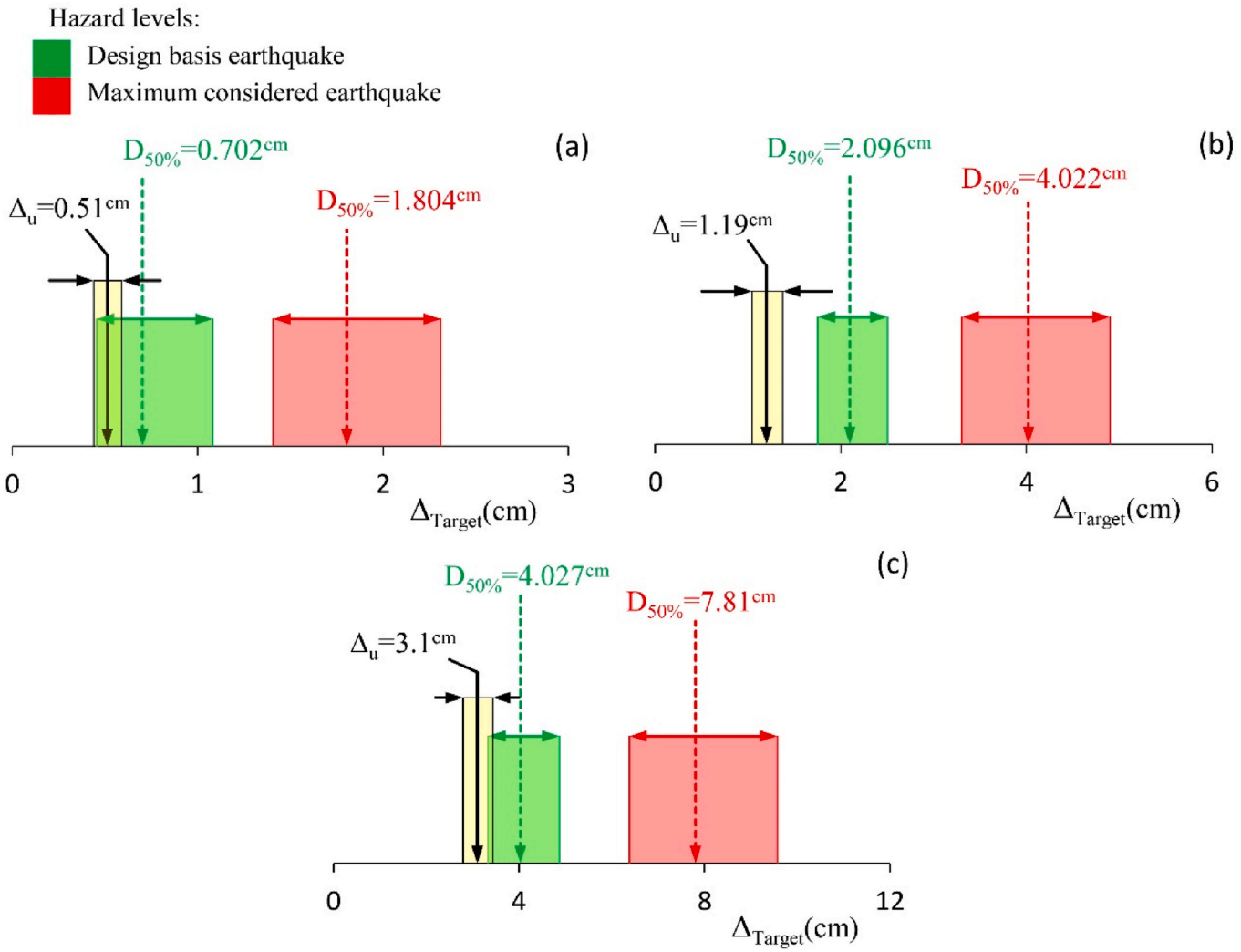

Fig. 27. Comparison of determined performance points by nonlinear time-history analysis (Δ_{Target}) and displacement amplification factor-based method (Δ_u) (a) 5-story building (b) 7-story building and (c) 10-story building.

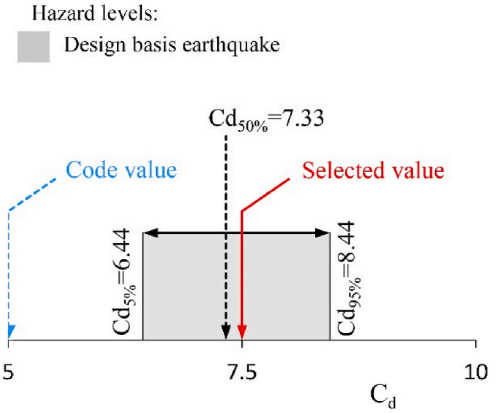

Fig. 28. Probabilistic range of displacement amplification factor (C_d) for tunnel-form system.

point under design basis earthquake in the 5-story building has been estimated at 27.35 % and for the 7- and 10-story buildings, 43.22 % and 23.02 % respectively (error exceeds 23 %). Due to this underestimation which is non-conservative for design purposes, the use of this method is also not recommended. Certainly, the existing error lies in the proposed C_d by the seismic design codes.

To compensate for this error, it is necessary to consider the tunnel-form system as an independent structural system and provide specific seismic design parameters for it. With the identification of response areas in both linear and nonlinear states (see Figs. 13 and 21), this factor can be easily extracted. According to Equation (12), the displacement amplification factor is defined as the ratio of displacements obtained from nonlinear time history analysis (Δ_{Target}) to the linear displacement (Δ_e).

$$C_d = \frac{\Delta_{Target}}{\Delta_e} \tag{12}$$

In probabilities of 5, 50 and 95 %, this ratio has been calculated for each building and the median value ($C_{d50\%}$) have been taken as the criterion for the system (see Fig. 28). According to Fig. 28, the displacement amplification factor in the tunnel-form system is definitely more than 5. Obviously, the values in the probability range of 50 and 95 % ($C_{d50\%} \leq C_d \leq C_{d95\%}$) are considered desirable with a higher confidence level. By considering the value of 7.5 for this factor, the probable range for the performance point will be as described in Fig. 29.

When the median values are considered ($D_{50\%}$ *and* Δ_u), compared to the accurate method, the prediction error of the performance point under design basis earthquake in the 5-story building has been limited to 10.54 %, and in the 7- and 10-story buildings, to 14.12 % and 15.47 % respectively. Although the response range is still narrower than the

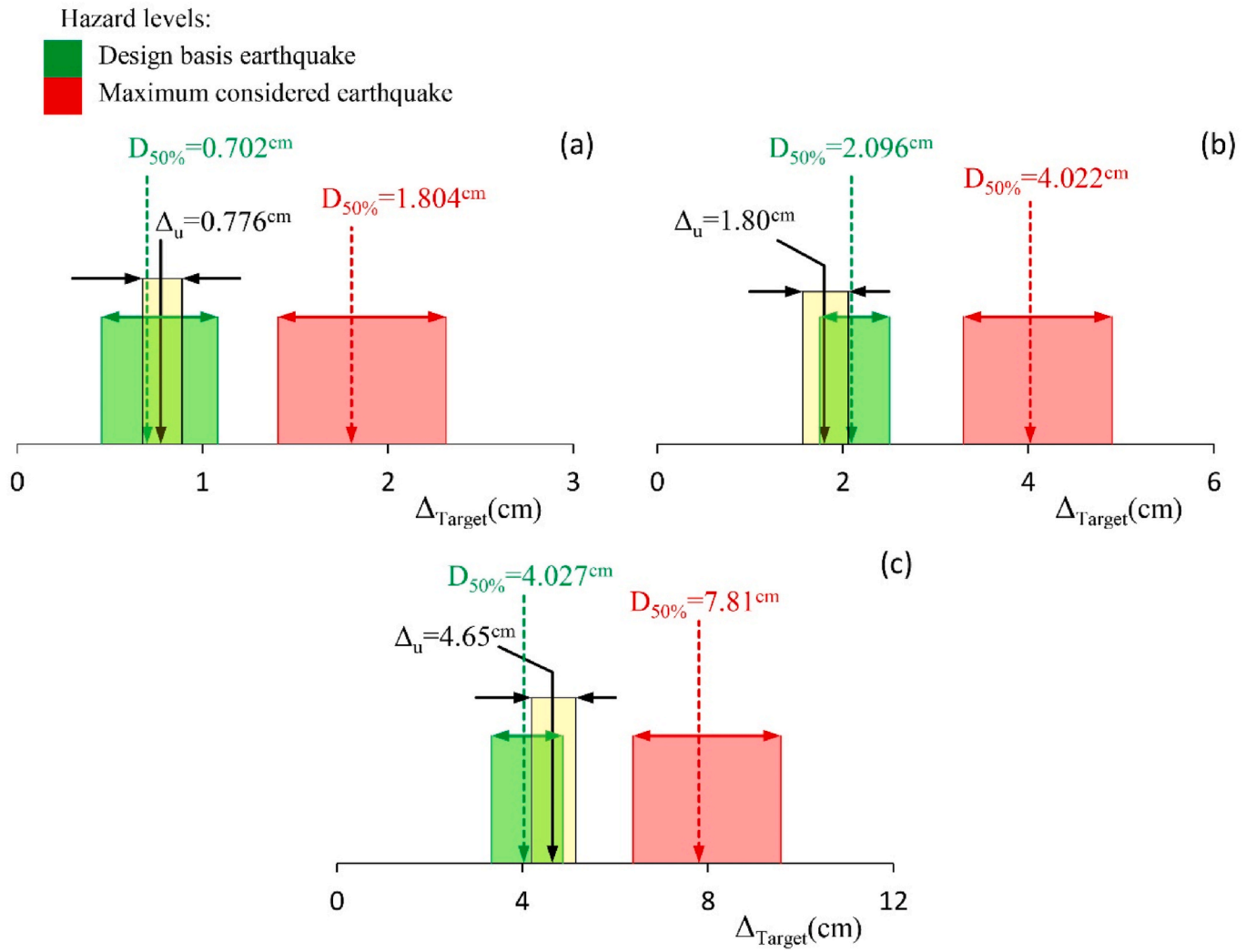

Fig. 29. Determined performance point after adjusting the displacement amplification factor (a) 5-story building (b) 7-story building and (c) 10-story building.

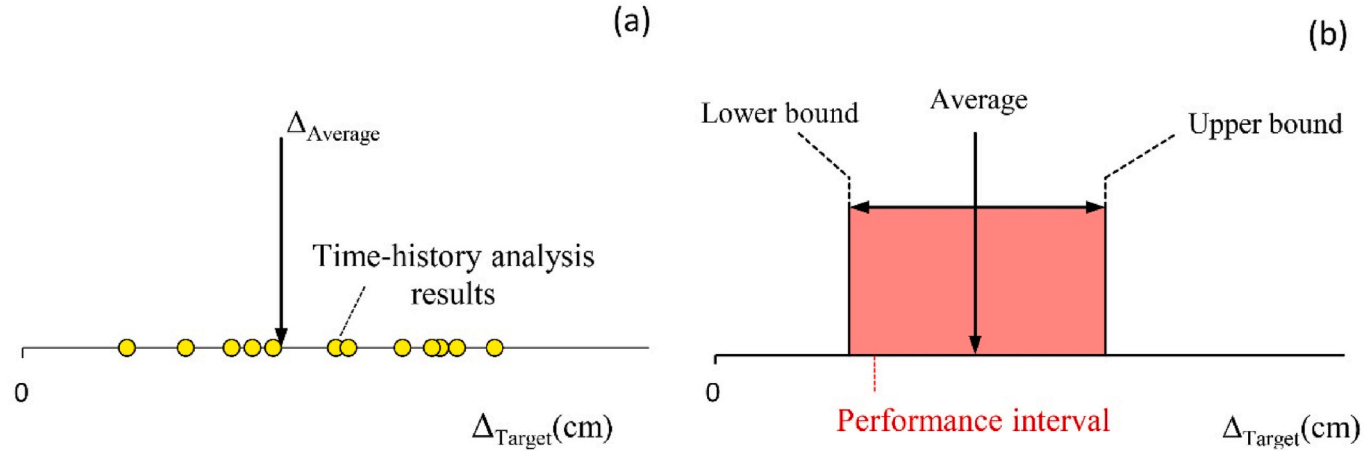

Fig. 30. Seismic performance evaluation using (a) Deterministic performance point (b) Probable Performance interval.

accurate method, the results have significantly improved. Based on the results; while extracting a specific C_d for tunnel-form system, this method can provide a more suitable estimation of the performance point, despite its simplicity.

6. Introducing the probable performance interval for seismic assessment

Even with similarities between records in terms of intensity and spectrum shape (see again Fig. 11), the performance point varies from

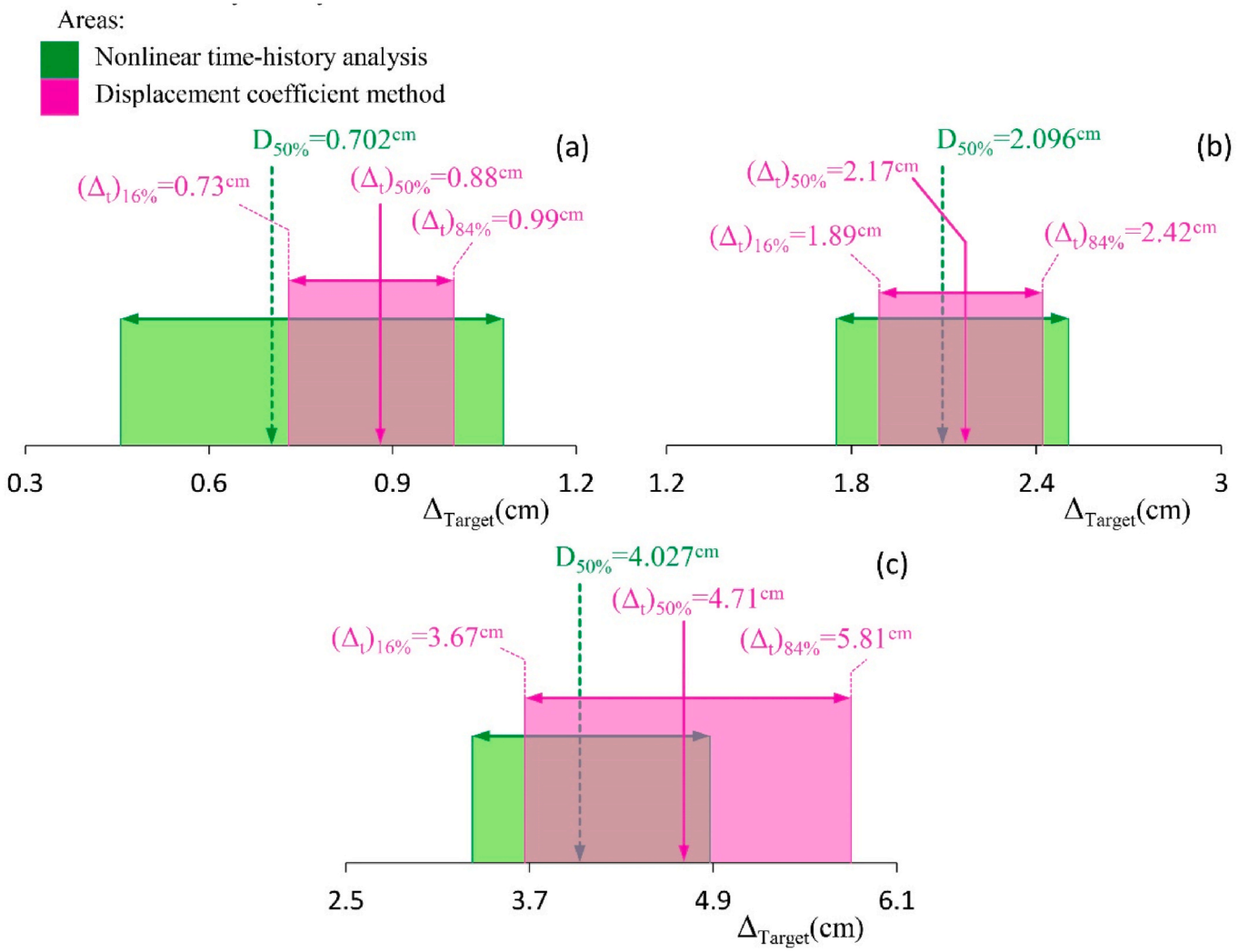

Fig. 31. Comparison of the probable performance intervals calculated from nonlinear time-history analysis and displacement coefficient method (a) 5-story building (b) 7-story building and (c) 10-story building.

one record to another. As shown in Fig. 30(a), considering the average response of all records ($\Delta_{Average}$) as a deterministic performance point is not reliable, as some responses exceed the average value.

It is observed that a deterministic performance point does not account for inherent uncertainties. In this context, as shown in Fig. 30(b), assessing the structure within the "Probable Performance interval" compensates for these challenges.

In this section, the " Probable Performance interval " parameter is introduced and its calculation details are explained. Subsequently, in a case study, this parameter is developed, and the tunnel-form system is evaluated under the design earthquake.

6.1. *Extracting the probable performance interval for tunnel-form buildings*

In all the methods described in Section 5, the performance point is presented deterministically. Given the extensive range of inherent uncertainties related to future earthquakes, a probabilistic approach is entirely reasonable.

According to the Iranian seismic design Code (Standard 2800) [22], in a pushover analysis, the building is pushed up to 1.5 times the calculated performance point, and within this range, a severe drop on the capacity curve is unacceptable.

Additionally, the code requires that at a displacement equivalent to 1.25 times the calculated performance point, the structure's strength must always be greater than the effective yield shear up to the target displacement.

Furthermore, at the performance point, a relative displacement of up to 1.2 times the allowable value is considered acceptable. It seems that the main goal of these provisions is to compensate for the challenges arising from inaccurate estimation of the performance point.

It is expected that using the "probable performance interval" parameter will address these challenges and relieve the user from controlling various provisions.

A probable performance interval for an earthquake encompasses a range of responses that very likely includes the structure's true performance point.

For the studied models, performance intervals have been extracted from detailed nonlinear time-history analysis for both design basis and the maximum considered earthquakes, as described in Subsection 4.1 (refer again to Figs. 12 and 13).

However, developing intervals through nonlinear time-history analysis is not practical for seismic performance evaluation using the pushover method.

Here, using a multi-level effective damping factor (β_e) is helpful. Since the uncertainties related to earthquakes are considered in calcu-

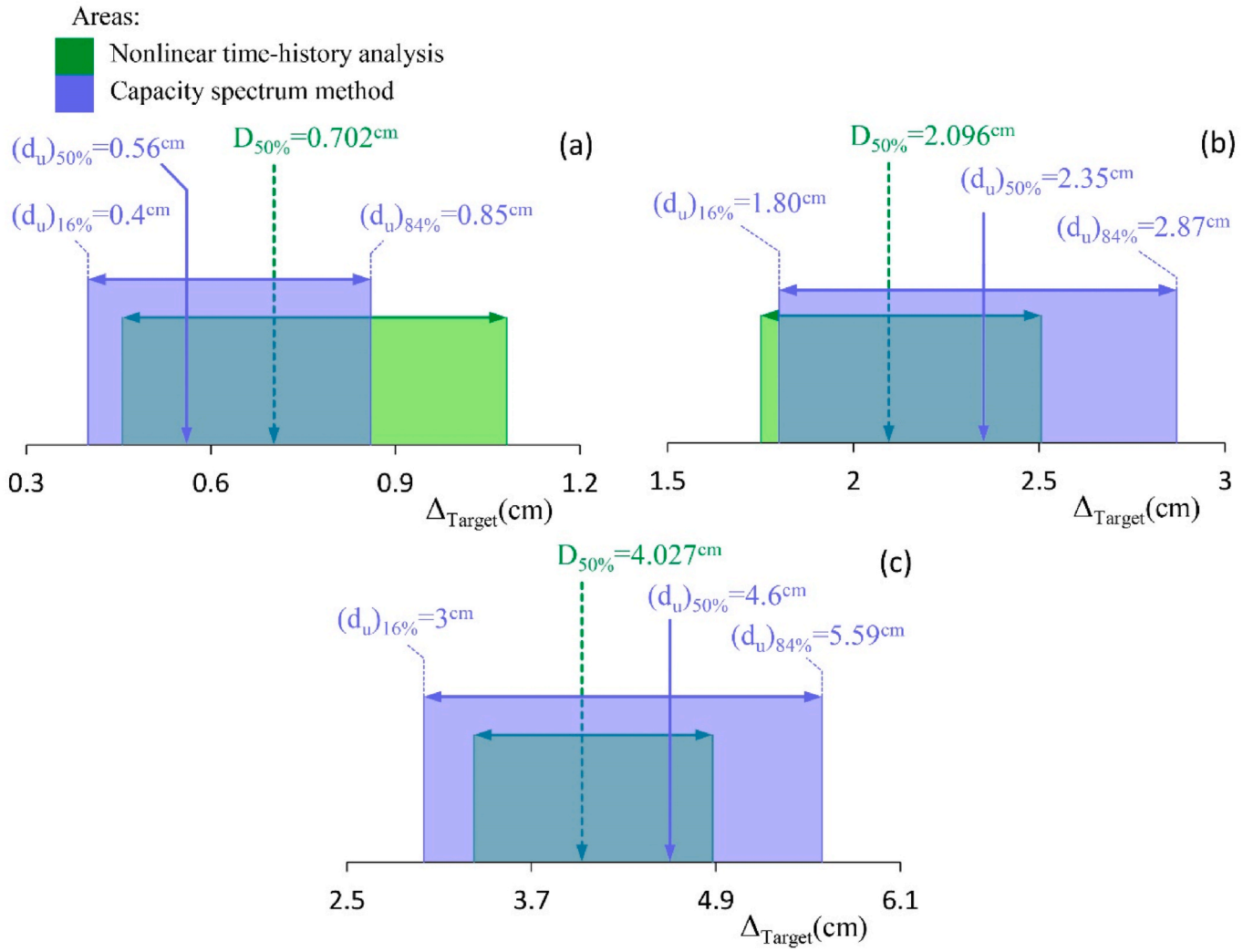

Fig. 32. Comparison of the probable performance intervals calculated from nonlinear time-history analysis and capacity spectrum method (a) 5-story building (b) 7-story building and (c) 10-story building.

lating the parameter β_e, it is expected that the prediction error will be satisfactorily reduced. Thus, the performance point corresponding to the 16th percentile of the structure's effective damping ratio is considered as the lower bound, while the 50th and 84th percentiles are considered as the median and upper bounds, respectively.

In the capacity spectrum method, to extract the performance point corresponding to a desired percentile, it is sufficient to substitute the damping corresponding to that percentile into Equation (6) and calculate the spectrum reduction factor (*SR*). In the next step, using the calculated reduction factor, the intersection of the reduced demand and capacity spectra in the *ADRS* system will be identified as the desired response (again see Figure (4)).

For displacement coefficient method, it is evident that for the effective period of the structure (T_e), the spectral acceleration (*Sa*) is obtained from the reduced demand spectrum with the effective damping corresponding to that percentile and used in the related calculations. Ultimately, the displacement calculated from Equation (1) will be the performance point corresponding to the mentioned percentile.

Developing the probable performance interval in the displacement amplification factor method also requires using different factors for C_d.

According to Fig. 28, when the C_d parameter corresponding to 5 %, 50 %, and 95 % probabilities is used for amplifying the lower, median and upper bounds of the elastic response range (refer to Fig. 21), the desired range will be extracted.

As shown in Figs. 31–33, under the design basis earthquake, the probable performance interval is calculated using the displacement coefficient method, capacity spectrum method and displacement amplification factor-based method and compared with the results of accurate nonlinear time-history analysis.

The investigations show that in all three methods, the developed probable interval adequately and reliably covers the probable response range under the design basis earthquake. As shown in Fig. 34(a), the probable performance interval for an earthquake has two bounds (i.e., Δ_L *and* Δ_U) and a median (i.e., *Average*). Thus, the performance interval can be divided into two different areas (i.e., *Zone* 1 and *Zone* 2). In a comparison, it is evident that the confidence level is higher in *Zone* 2.

With the aim of designing the structure under this earthquake, it is obvious that a severe drop in capacity curve within the entire interval ($\Delta_L \leq \Delta \leq \Delta_U$) is not permissible (see Fig. 34(b)). Moreover, considering the median range (*Average*) as the target, it is recommended that the structure's strength always be greater than the yield strength (V_y) within the range between the median and upper bound (i.e., *Zone* 2).

With the aim of evaluating the seismic performance of the structure, the desired performance level must be met throughout the entire range (see Fig. 34(c)). If, based on local failure criteria, the desired performance level is violated in some elements, a design review would be necessary. For evaluation purposes, the responses at the upper bound (Δ_U) will be used.

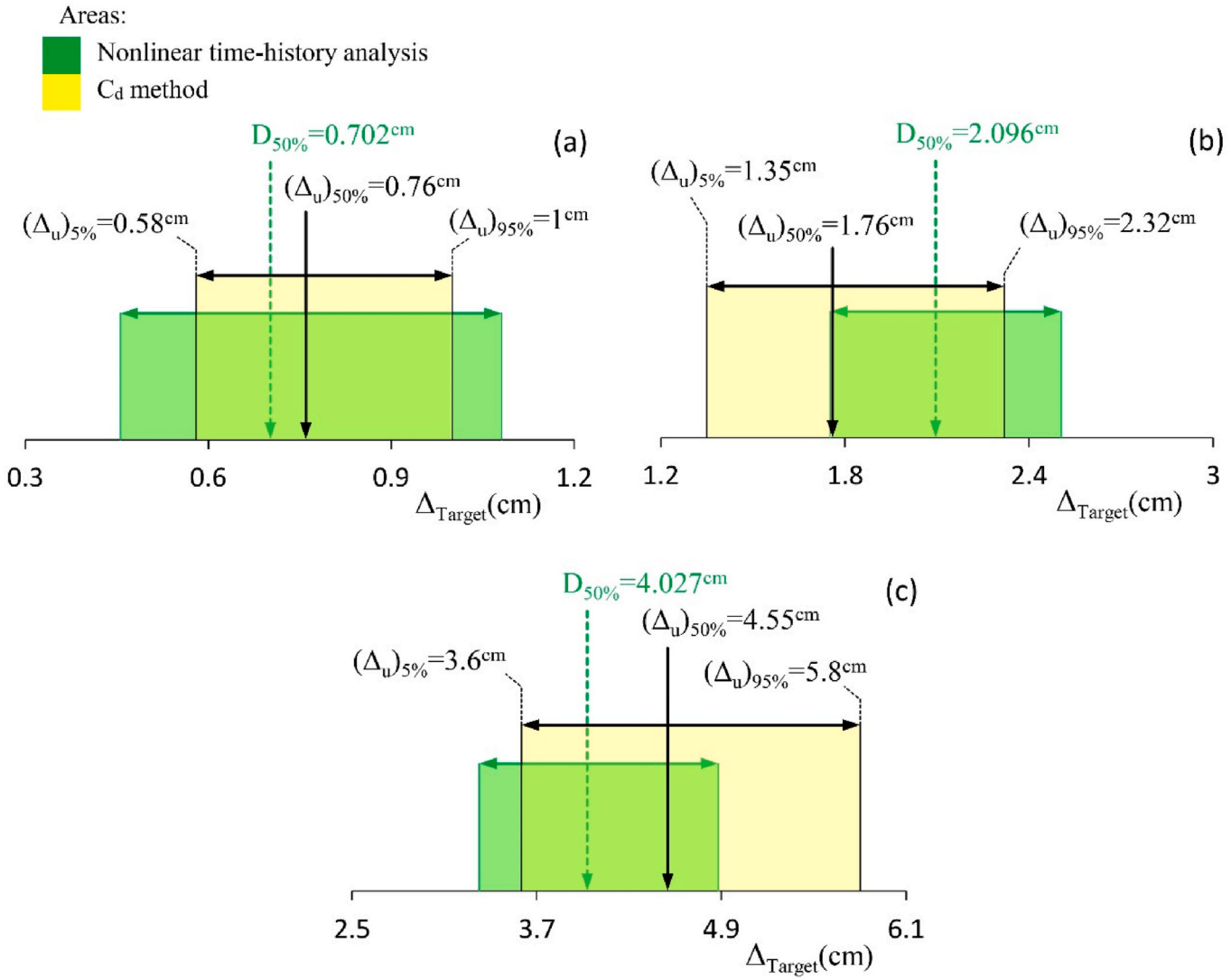

Fig. 33. Comparison of the probable performance intervals calculated from nonlinear time-history analysis and displacement amplification factor-based method (a) 5-story building (b) 7-story building and (c) 10-story building.

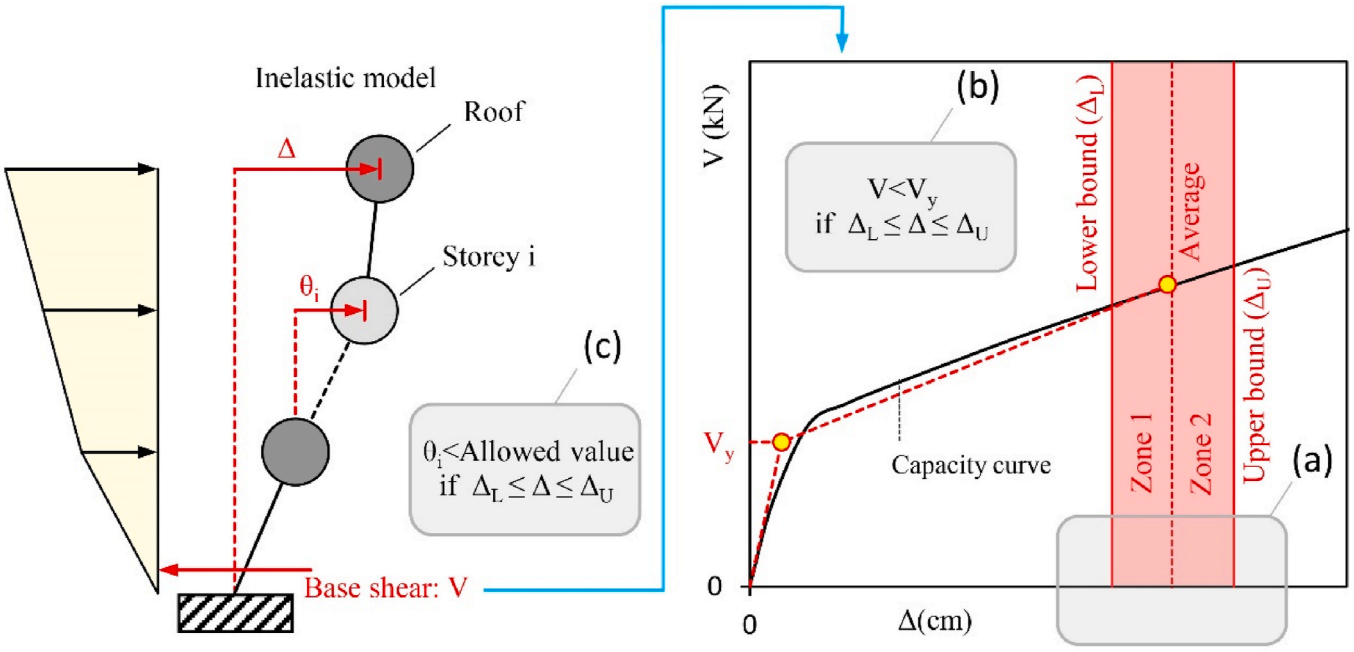

Fig. 34. Pushover analysis of a hypothetical model and its evaluation (a) Probable performance interval (b) Strength control (c) Seismic performance control.

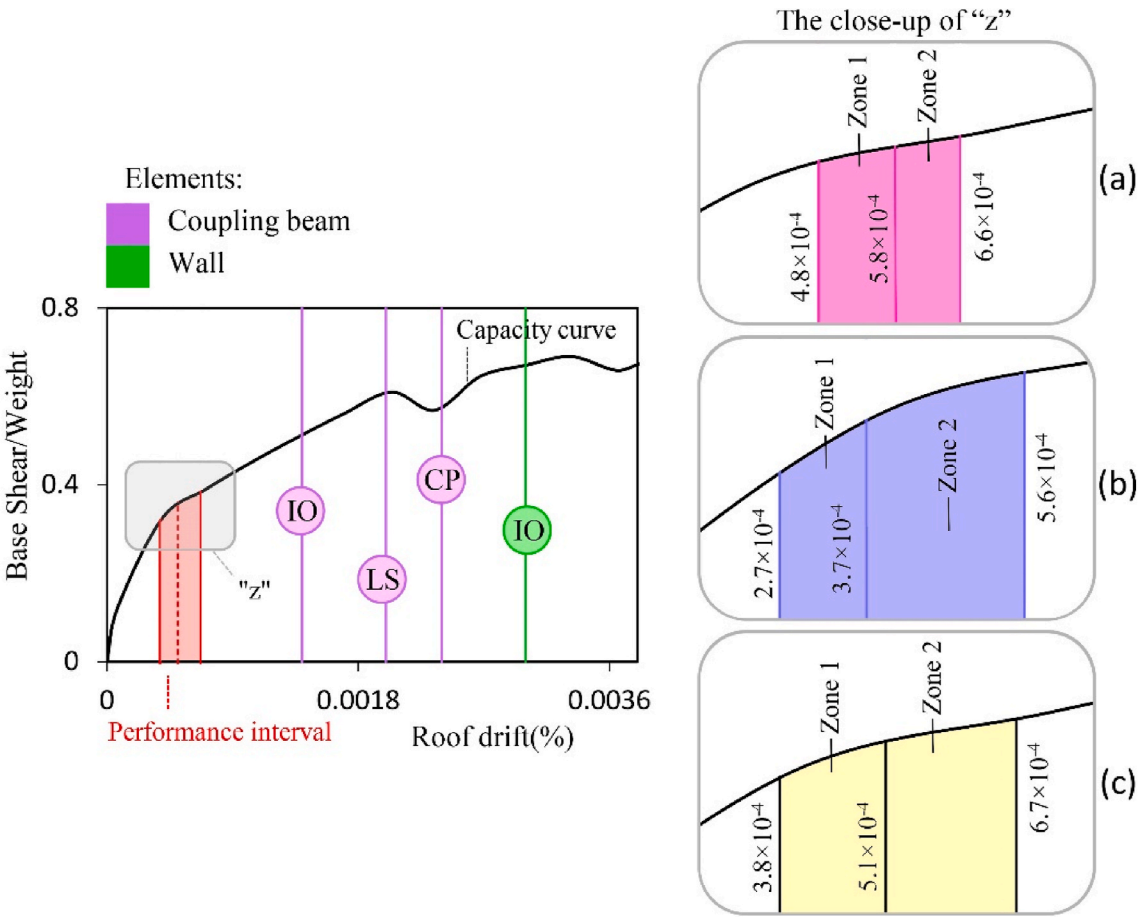

Fig. 35. Capacity curve for a 5-story building, failure states and performance interval extracted using different methods (a) Displacement coefficient method (b) Capacity spectrum method and (c) Displacement modification factor-based method.

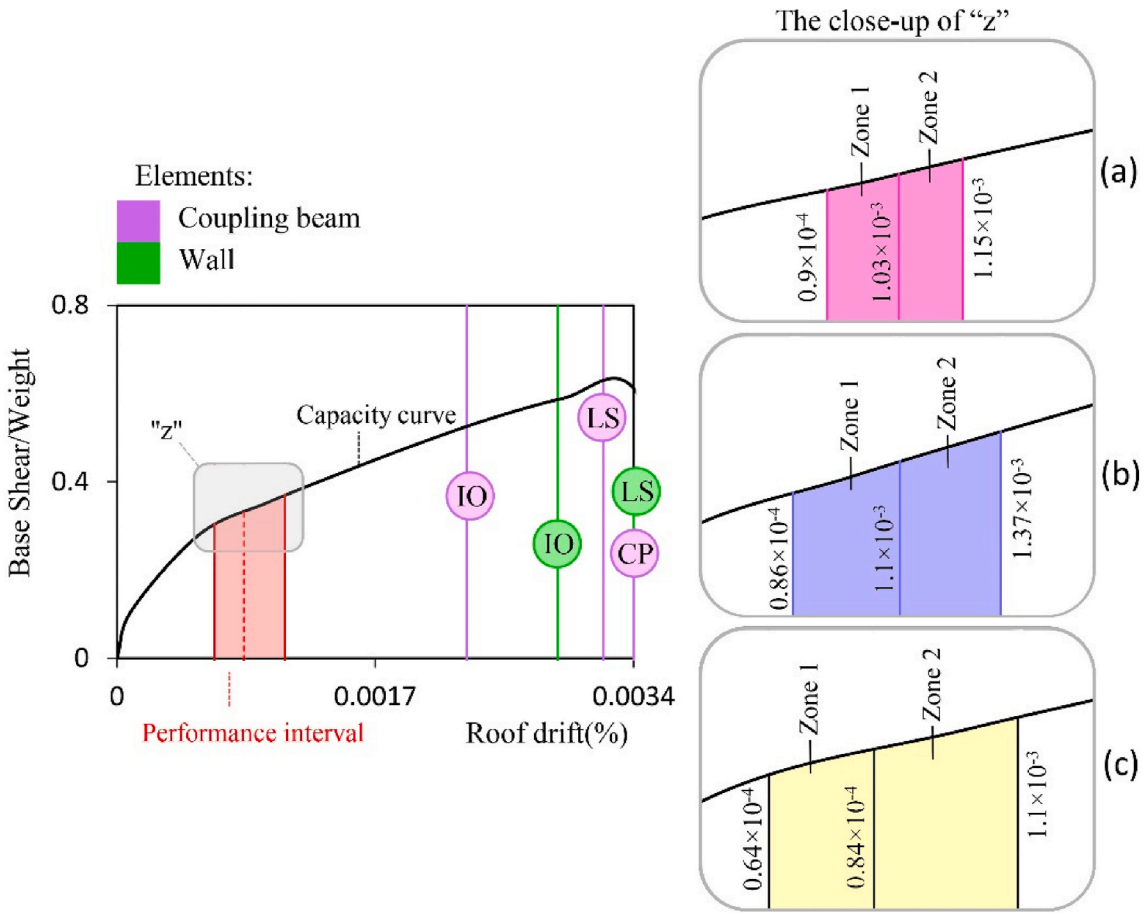

Fig. 36. Capacity curve for a 7-story building, failure states and performance interval extracted using different methods (a) Displacement coefficient method (b) Capacity spectrum method and (c) Displacement modification factor-based method.

6.2. Evaluating the tunnel-form system in the probable performance interval

According to Figs. 35–37, the seismic behavior of the system was assessed using the pushover method and the probable performance interval. In the evaluation process, the probable performance interval extracted by all three methods (Figs. 31–33) was used to determine their accuracy in estimating the seismic behavior. The figures show that the performance interval in all three methods provides a similar estimation of the system's performance level.

As observed, under the Design Basis Earthquake (*DBE*), walls and coupling beams are remained at a level higher than Immediate Occupancy (IO) performance level. Additionally, in *Zone* 2 of each performance interval, the capacity curves are always rising, and lateral strength exceeds yield strength. Thus, no significant problem or considerable damages to the system are expected when subjected to the *DBE*.

Subsequently, responses of inter story drift ratio and story shear force were measured and compared up to the upper bound of each interval (see Figs. 38 and 39). Figs. 38 and 39 show that in all three methods, the vertical distribution of force and displacement responses at the upper bound of the interval are also very close to each other.

In summary, it is evident that the development of the probable performance interval using all three methods yields desirable and close results. Additionally, using this parameter exempts the user from additional controls.

7. Discussion and conclusion

The present study aims to evaluate the accuracy of displacement coefficients, capacity spectrum, and displacement amplification factor-based methods in estimating the performance point of cast-in-place tunnel-form concrete buildings under design basis earthquake. A hierarchical structure is detailed for each method in the text. By considering the results obtained from nonlinear time-history analysis as the precise response, the error of each method has been calculated and reported. Based on findings, weaknesses are inherent in each method. In some methods, the prediction error is significant to the extent that their use under current conditions is not recommended at all. Furthermore, after identifying primary weaknesses and error-generating parameters, corrections have been proposed for each method. Based on the results, using desirable values of effective damping ratio and displacement amplification factor for the system can significantly improve the results.

For the first time in this study, the concept of " probable performance interval" has been proposed instead of "performance point". This parameter, a simple yet effective factor, compensates for inherent uncertainties related to future earthquakes and details have been presented for its development. Within the scope of the models examined and the assumptions adopted, the key study findings are as follows.

- Under the design basis earthquake, the effective damping ratio (β_e) in some earthquake records exceeds 30 % ($\beta_e \geq 30^{\%}$). According to the ATC-40 classification, the behavior in the tunnel-form system is of type A (excellent quality).
- In estimating the performance point of the tunnel-form system, the displacement coefficient method is highly inefficient, with an error

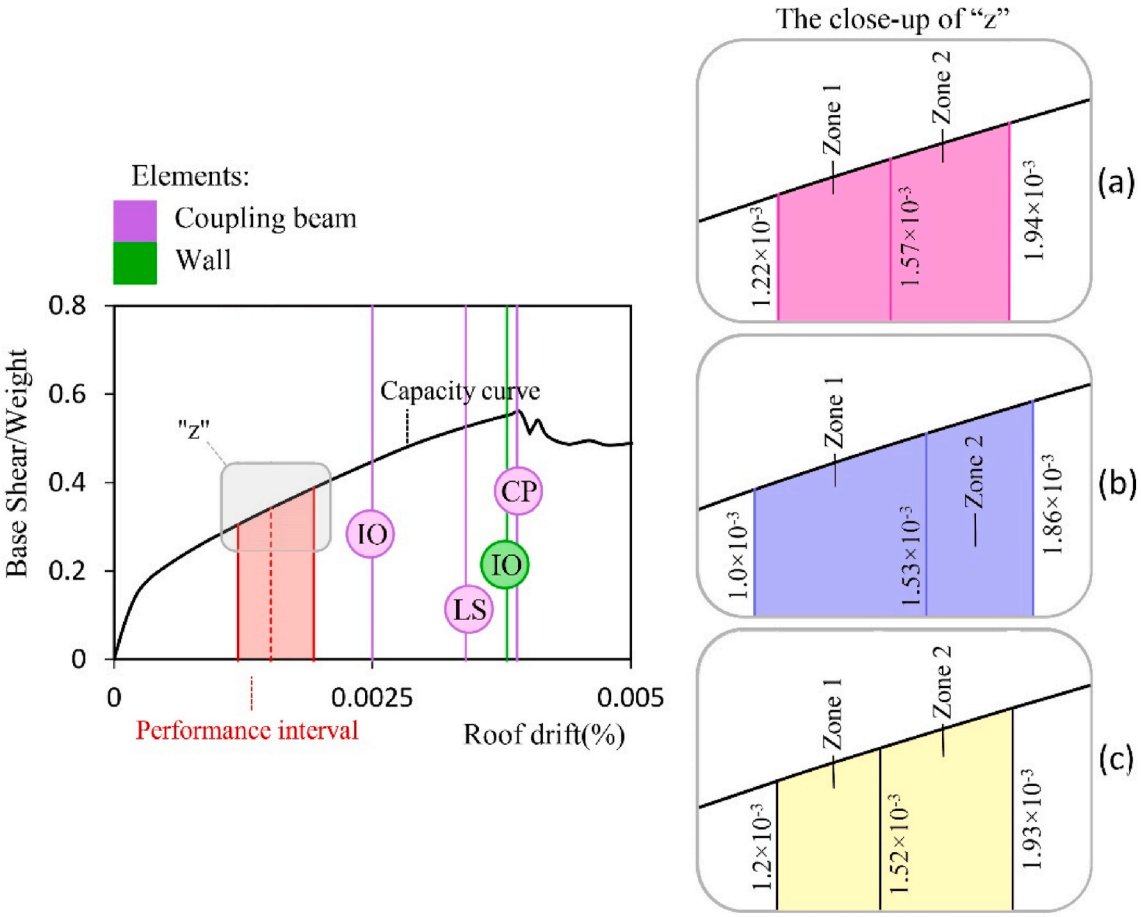

Fig. 37. Capacity curve for a 10-story building, failure states and performance interval extracted using different methods (a) Displacement coefficient method (b) Capacity spectrum method and (c) Displacement modification factor-based method.

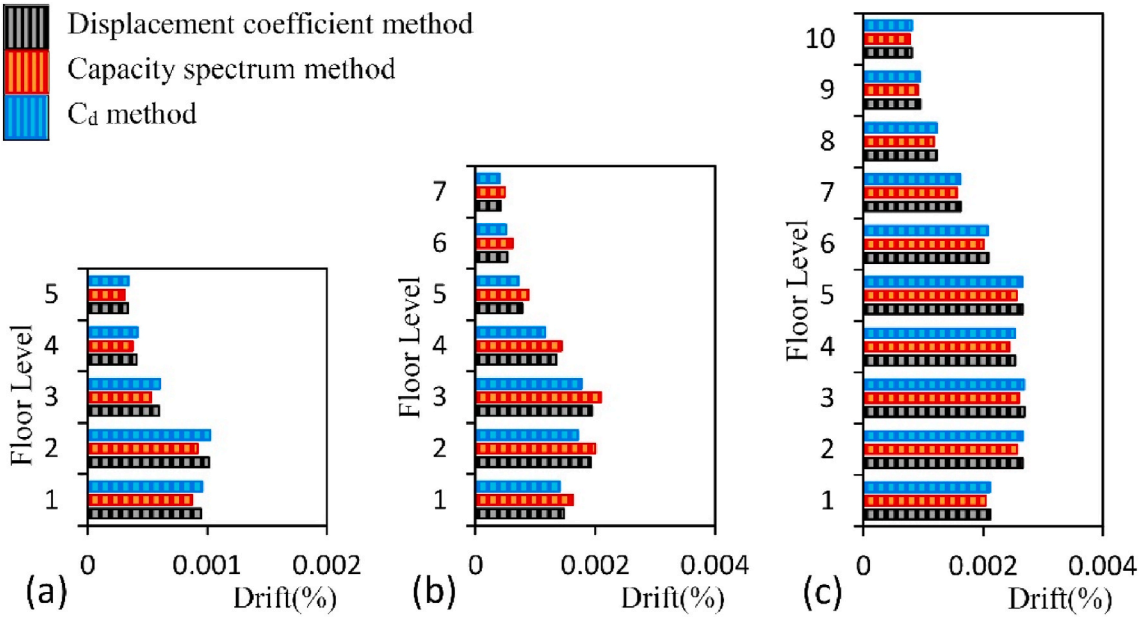

Fig. 38. Estimation of inter story drift ratio at the upper bound during pushover analysis in buildings (a) 5-story (b) 7-story and (c) 10-story.

exceeding 80 %. The response in this method is much greater than reality and close to the system's response under the maximum considered earthquake. The spectral acceleration corresponding to the effective period at 5 % damping ($Sa(T_e\&5\%)(g)$) has been identified as the main source of error, and replacing it with the spectral

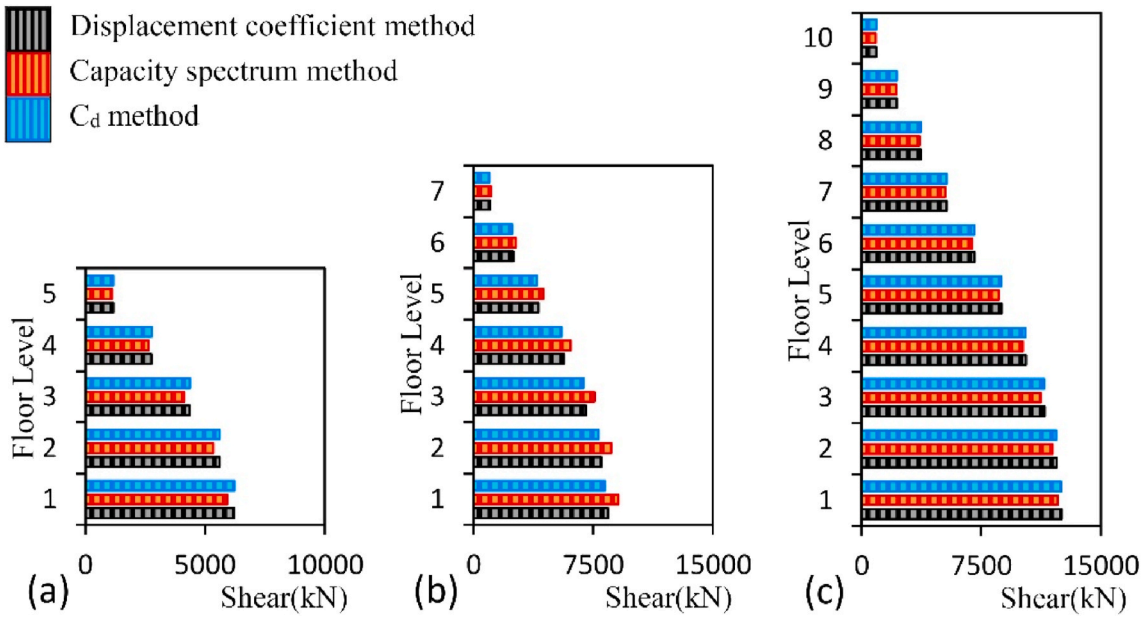

Fig. 39. Estimation of story shear force at the upper bound during pushover analysis in buildings (a) 5-story (b) 7-story and (c) 10-story.

acceleration corresponding to the effective period at effective damping ($Sa(T_e\&\beta_e\%)(g)$) has been proven as a corrective approach.

- The capacity spectrum method, which is based on trial and error, is time-consuming. However, by using the effective damping of the system in the calculation process, this method provides acceptable results in a single attempt without iterative processes. The estimation of this method for the system's performance point is within the probable range and towards safety.
- The method based on the displacement amplification factor underestimates the system's performance point with more than 23 % error, which is non-conservative. In this method, the displacement amplification factor (C_d) has been identified as the main error source. Probabilistic assessments showed that this parameter is 100 % higher than the value suggested by the code (5). Using the value of 7.5, with a confidence level of nearly 50 %, significantly reduced the error in this method.
- In the pushover analysis of the system, the probable performance interval is a desirable parameter for addressing the inherent uncertainties related to earthquakes and can be developed using all three methods (i.e., displacement coefficients, capacity spectrum and displacement amplification factor-based). The seismic performance and system responses (both force and displacement) in all three methods were closely aligned with high accuracy.

In addition to the characteristics of the input motions, it is evident that the modal properties of the system also significantly affect the results. Therefore, further studies aimed at assessing the influence of effective parameters on the results of the mentioned methods (including the relative wall area in the plan, building height, irregularities in plan and height, foundation flexibility and changes in the frequency content of the records) are suggested.

In this study, the damping ratio, independent of the performance level in the structural elements, was only provided for the design basis earthquake. Dividing this parameter into demand (specific hazard levels for the site) and capacity (specific performance levels in the lateral resisting system) allows for estimating the system's performance point at desired levels of earthquake intensity. Based on these explanations, providing multi-level effective damping parameters for tunnel-form system can serve as a suitable basis for future studies.

The evaluation of seismic performance using the pushover method, with the help of the probable performance interval parameter, is independent of the structural system and applicable to other lateral resisting systems as well. Assessing the adequacy of this parameter in estimating the seismic behavior of various structural systems and comparing it with fragility and incremental dynamic analyses can also be a suitable research area for researchers.

CRediT authorship contribution statement

Vahid Mohsenian: Writing – original draft, Methodology, Investigation, Formal analysis, Conceptualization. **Luigi Di-Sarno:** Writing – review & editing, Visualization, Validation, Supervision, Project administration, Methodology, Investigation, Conceptualization.

Declaration of competing interest

I can declare on behalf of my coauthor that we have no conflicting interests regarding submission of this manuscript to Soil Dynamics and Earthquake Engineering.

Data availability

Data will be made available on request.

Acknowledgments

The authors express their gratitude to Dr. Egemen Sönmez for sharing the images obtained from the earthquake experiences and damages of the 2023 Turkey earthquakes.

References

[1] Mohsenian V, Filizadeh R, Nikkhoo A, Hajirasouliha I. Multi-level response modification factors for performance-based seismic design of tunnel-form building structures. J Earthq Eng 2023;27(15):4288–305.
[2] Mohsenian V, Gharaei-Moghaddam N, Hajirasouliha I. Seismic performance assessment of tunnel form concrete structures under earthquake sequences using endurance time analysis. J Build Eng 2021;40(2021):102327.
[3] Balkaya C, Kalkan E. Seismic vulnerability, behavior and design of tunnel form building structures. Eng Struct 2004;26(14):2081–99.
[4] Pujol S, Bedirhanoglu I, Donmez C, Dowgala JD, Eryilmaz Yildirim M, Klaboe K, Koroglu FB, Lequesne RD, Ozturk B, Pledger L, Sonmez E. Quantitative evaluation of the damage to RC buildings caused by the 2023 southeast Turkey earthquake sequence. Earthq Spectra 2024;40(1):505–30.

[5] IBHRC. Approved technologies indirection of sub-note 2-6, paragraph "D", Note 6, "A step in direction of building industrialization. first ed. Building and Housing Research Center Press; 2007. p. 21–2.
[6] Yuksel SB, Kalkan E. Behavior of tunnel form buildings under quasi-static cyclic lateral loading. Struct Eng Mech 2007;27(1):99–115.
[7] Brunesi E, Peloso S, Pinho R, Nascimbene R. Cyclic testing and analysis of a full-scale cast-in-place reinforced concrete wall-slab-wall structure. Bull Earthq Eng 2018;16(2):4761–96.
[8] Goel RK, Chopra AK. Period formulas for concrete shear wall buildings. J Struct Eng 1998;124(4):426–33.
[9] Lee LH, Chang KK, Chun YS. Experimental formula for the fundamental period of RC buildings with shear-wall dominant systems. Struct Des Tall Build 2000;9(4):295–307.
[10] Balkaya C, Kalkan E. Estimation of fundamental periods of shear-wall dominant building structures. Earthq Eng Struct Dynam 2003;32(7):985–98.
[11] Balkaya C, Yuksel SB, Derinoz O. Soil-structure interaction effects on the fundamental periods of the shear-wall dominant buildings. Struct Des Tall Special Build 2012;21(6):416–30.
[12] Mohsenian V, Nikkhoo A, Rostamkalaee S, Moghadam A, Hejazi F. The seismic performance of tunnel-form buildings with a non-uniform in-plan mass distribution. Structures 2020;29(2021):993–1004.
[13] Mortezaei A, Mohsenian V. Reliability-based seismic assessment of multi-story box system buildings under the accidental torsion. J Earthq Eng 2019;26(2):674–97.
[14] Mohsenian V, Hajirasouliha I, Mariani S, Nikkhoo A. Seismic reliability assessment of RC tunnel-form structures with geometric irregularities using a combined system approach. Soil Dynam Earthq Eng 2020;139:106356.
[15] Mohsenian V, Nikkhoo A. A study on the effects of vertical mass irregularity on seismic performance of tunnel-form structural system. Advances in Concrete Construction 2019;7(3):131–41.
[16] Tavafoghi A, Eshghi S. Evaluation of behavior factor of tunnel-form concrete building structures using Applied Technology Council 63 methodology. Struct Des Tall Special Build 2013;22(8):615–34.
[17] Mohsenian V, Gharaei-Moghaddam N, S Moghadam A. Exploring the distribution of seismic loads in tunnel-form concrete buildings using the probable area method. Results in Engineering 2024;21(2024):101851.
[18] Beheshti-Aval SB, Mohsenian V, Sadegh-Kouhestani H. Seismic performance-based assessment of tunnel form buildings subjected to near- and far-fault ground motions. Asian Journal of Civil Engineering 2018;19(1):79–92.
[19] Mohsenian V, Nikkhoo A, Hejazi F. An investigation into the effect of soil-foundation interaction on the seismic performance of tunnel-form buildings. Soil Dynam Earthq Eng 2019;125:105747.
[20] Mohsenian V, Mortezaei A. Effect of steel coupling beam on the seismic reliability and R-factor of box-type buildings. Structures and Buildings 2019;172(10):721–38.
[21] Mohsenian V, Nikkhoo A, Hajirasouliha I, Hejazi F. A low computational cost seismic analyses framework for 3D tunnel-form building structures. Adv Struct Eng 2022;0(0):1–15.
[22] Permanent Committee for Revising the Standard 2800. Iranian code of practice for seismic resistant design of buildings. fourth ed. Tehran, Iran: Building and Housing Research Center; 2014.
[23] ASCE. Minimum design loads and associated criteria for buildings and other structures, ASCE/SEI 7-22. American Society of Civil Engineers 2022. Reston, Virginia.
[24] ASCE/SEI 41-17. Seismic evaluation and retrofit of existing buildings. Reston, VA: American Society of Civil Engineers; 2017.
[25] Applied Technology Council. Seismic evaluation and retrofit of concrete buildings, ATC-40 report, vols. 1 and 2. Redwood City, California: Report No. ATC-40; 1996.
[26] FEMA 440 Report. Improvement of nonlinear static seismic analysis procedures. Washington, D.C., U.S: Federal Emergency Management Agency; 2005.
[27] Anil K, Chopra. Dynamics of structures: theory and applications to earthquake engineering. fourth ed. 2011.
[28] Mohsenian V. R-factor determination for tunnel-form buildings, MS. Thesis. Iran, Tehran: University of Science and Culture; 2013 (in Persian).
[29] American Concrete Institute. Building code requirements for structural concrete (ACI 318-19). Farmington Hills, MI: ACI; 2019.
[30] Computers and Structures Inc. (CSI). Structural and earthquake engineering software. Berkeley, CA, USA: ETABS, Extended Three Dimensional Analysis of Building Systems Nonlinear; 2015., Version 15.2.2.
[31] Paulay T, Binney JR. Diagonally reinforced coupling beams of shear walls. Shear in Reinforced Concrete, ACI Special Publications 1974;42:579–98.
[32] Zhao ZZ, Kwan AKH, He XG. Nonlinear finite element analysis of deep reinforced concrete coupling beams. Eng Struct 2004;26(1):13–25.
[33] Computers and Structures Inc. (CSI). Structural and earthquake engineering software. Berkeley, CA, USA: PERFORM-3D Nonlinear Analysis and Performance Assessment for 3D Structures; 2016., Version 6.0.0.
[34] Mohsenian V, Di Sarno L. Numerical analysis of potential failure modes in shear walls of the tunnel form concrete system: performance-based approach. Eng Struct 2024;303(2024):117494.
[35] Technical Criteria Codification and Earthquake Risk Reduction Affairs Bureau. Instruction for seismic rehabilitation of existing buildings. Iran: Management and Planning Organization; 2014. No. 360, 2nd edition.
[36] Hancock J, Watson-Lamprey J, Abrahamson NA, Bommer JJ, Markatis A, McCoy E, Mendis R. An improved method of matching response spectra of recorded earthquake ground motion using wavelets. J Earthq Eng 2006;10:67–89.
[37] https://seismosoft.com/.
[38] PEER Ground Motion Database, Pacific Earthquake Engineering Research Center, Web Site: https://ngawest2.berkeley.edu/; Accessed: Jan 2021.
[39] Mohsenian V, Gharaei-Moghaddam N, Arabshahi A. Evaluation of the probabilistic distribution of statistical data used in the process of Developing fragility curves. International Journal of Steel Structures 2022;22(4):1002–24.
[40] Mohsenian V, Hajirasouliha I, Filizadeh R. Seismic reliability assessment of steel moment-resisting frames using Bayes estimators. Structures and Buildings 2023;176(4):306–20.
[41] Meng J-Y, Lu D-G, Shan B-H. Probabilistic-based seismic fragility assessment of earthquake-induced site liquefaction. Soil Dynam Earthq Eng 2023;175:108250.
[42] Norouzi A, Poursha M, Amini MA. Seismic collapse fragility analysis of steel moment-resisting frames (MRFs) with stiffness and strength deterioration considering the spectral shape of ground motion records. Soil Dynam Earthq Eng 2024;183:108781.